School of Computing, Engineering and Mathematics

Division of Engineering and Product Design

Super Regenerative Radio Receivers

Luke Alexander Pilgrim

XE336

Supervised by: Dr. Simon Busbridge

May 2016

Final year report submitted in partial fulfilment of the requirements for the degree of BEng (Hons) Electronic & Electrical Engineering

DISCLAIMER

I hereby certify that the attached report is my own work except where otherwise indicated. I have identified my sources of information; in particular I have put in quotation marks any passages that have been quoted word-for-word, and identified their origins.

Signed ……

Date ……

Acknowledgments

The author would like to express their utmost gratitude to Dr Simon Busbridge and Dr Deshinder Gill Singh for all the support and knowledge on the field of RF they have shared. The author would also like to thank all staff at the University of Brighton for making this project possible.

Abstract

This document details the research, design process and construction process of a super-regenerative Receiver. A super-regenerative receiver (SRR) is a device which detects and demodulates radio signals. This document analyses the design of transistor based SRRs. The objective is to modify the design of an existing SRR then design, simulate and construct a working circuit. During this process, several of the key operating parameters of an SRR were observed. From the observations made during simulation and testing, ways of improving the design shall be noted as well as some of the fundamental flaws of SRRs. Key to the operation of an SRR is a type of waveform known as a 'quench'. Analysing the purpose and effects of quench is a key objective of this project. SRR's come in two main types, self-quenching and externally quenched. One of the main objectives of this project is to simulate both a self-quenching and an externally quenched circuit and observe the differences between the two.

Contents

List of Figures

List of Tables

Chapter 1.0 – Project Introduction

1.1 Overview of project

The main objective of this project is to construct and test a super-regenerative radio receiver. The super-regenerative receiver (SRR) is a type of radio receiver, designed in 1922 by the American Engineer Edwin H. Armstrong. Original designs of SRR were based around the use of thermionic valves to amplify minute radio signals then demodulate them back into the audio signal which they carry. Later designs of SRR incorporated transistors instead of valves, and one of the main objectives of this project is to analyse the design of these transistor based receiver circuits. This is to be done using both simulation software and the construction and testing of a physical circuit. The results obtained from these tests will then be used to prove some of the fundamental mathematical and physical concepts and theories behind the operation of a super regenerative receiver.

The construction of a physical circuit will be based around an existing design, however, necessary modifications will be made in an attempt to better the performance of the circuit. Super regenerative radio receivers have several variations in their design and modes of operation. The two most fundamental designs of SRR are self-quenching circuits and circuits with an external quenching oscillator. The concept of quench will be discussed later in this document. The 2 main modes of operation utilized by SRR's are linear quench and logarithmic quench. This document will deal mainly with the concept of linear mode quench, and the usage of different types of wave (sine, saw tooth, square wave) to implement this quench.

The super regenerative receiver is not commonly used in this day and age, as it fell out of favour to other radio designs, such as the superhetrodyne radio receiver. The SRR has several downfalls, most notably it tendency to cause interference with other nearby radio equipment, due to its oscillator producing RF radiation. Another drawback to this type of receiver is the fact that it was notoriously difficult to tune, which made it unable to compete with more modern, easier to tune radios. Despite this, the super regenerative receiver has several merits, most notably its incredible simplicity and low energy usage. An SRR can be constructed with a very small handful of components, making them incredibly cheap to manufacture. A low component count can also help

make the unit much smaller than more elaborate designs with a higher component count.

These merits have allowed the usage of the SRR to continue in a number of different functions apart from just audio communications broadcast, which it was originally designed for, for instance, simple radio controlled devices such as doorbells and electrical garage door opening mechanisms. This document will also explore further applications of SRR as well as possible future purposes for this type of receiver.

1.2 Reason for choosing this project

RF devices are a staple part of modern technology, with new applications for it being devised all the time. Despite the evolution of digital audio broadcast and internet radio, the classic types of radio, AM and FM receivers still remain widely used. An increasing number of mobile phones are capable of acting as FM/AM radios, and the rise of Ultra High Frequency (UHF) channels has allowed radio to become an effective method of transmitting digital images and data as well as just analogue audio and video signals. The basic design of the SRR has been utilized recently for the reception of digital data signals. The simplicity of an SRR's design makes it a good test bench with which to study the principles of receiving RF signals. This is because the SRR has the ability to receive both AM and FM signals, unlike some other designs of radio, which require a separate receiver for the different types of signal.

1.3 Project Aims and Objectives

1.3.1 Aim

The main aim of this project is to analyse the design of an SRR, then build and test it. This project aims to create a radio receiver which operates in linear mode and can detect Band II VHF frequencies. VHF signals are commonly used in amateur radio, the broadcast of commercial FM radio and aircraft band AM communication signals. VHF ranges from 30 MHz to 300MHz in frequency. Band II is the most widely used part of this spectrum and stretches between 88 and 108 MHZ. This is the part of the spectrum on which all commercial FM stations operate. This range of frequencies will be the main range of operation for the super regenerative receiver. In order to receive on this band width, the receiver must be designed in an appropriate manner to detect

the required frequency. Once the SRR circuit has been completed and tested, the results are to be analysed and compared to the super regenerative theory outlined in the research material.

1.3.2 Objectives

Objective 1: Simulation. This project will utilise the simulation package LT spice. Once a suitable design has been selected, it will be constructed and tested on LT spice. LT spice is capable of carrying out several modes of simulation. The most widely utilized ones in this project will be Transient analysis, D.C operating point, A.C. analysis, Thermal noise and Transfer function. These different modes of simulation will be used to analyse the waveforms, currents and voltages generated in the circuit. Simulations will be carried out several times, each time the circuit will have a slightly different set of component values. This set of tests aims to observe the difference made on the waveforms, currents and voltages as a result of these changes in component value. Both a self-quenching and externally quenched circuit will be analysed, as well as simulations trying different type of waveforms as an external quench. Simulations will also allow the effects of any modifications made to the design to be observed. Once an appropriate set of results have been acquired, the design used in the simulation and its corresponding component values will be applied to the next objective, construction of a circuit.

Objective 2: Construct and test a tuned oscillator circuit. The oscillator circuit is a simple resonant circuit, constructed using an inductor (L), a variable capacitor (C) attached via the collector to an NPN transistor with a resistor(R) attached at its emitter and a capacitor across the collector and emitter. The purpose of this circuit is to produce a sinusoidal voltage which can have its frequency adjusted by varying the capacitance. The main objective at this stage is to get the oscillator to oscillate between 88-108MHz.

Objective 3: **Construct and test the resonant circuit.** The resonant circuit is attached to either the base or the emitter of the transistor in the tuned oscillator (in this example it is attached to the emitter). The resonant circuit is the part of the SRR responsible for detecting the RF frequencies. It is also creates the phenomenon known as “quench”. Quench can be initiated by both thermal noise in the system, and by stimulation from

a radio signal. In this stage the output from the circuit will be grounded and no RF will be applied. The main objective at this stage is to observe the behaviour of the wave forms at the base, collector and emitter of the transistor. The waveforms from the output shall also be observed using an oscilloscope. This test is to be repeated with the tuned oscillator set to oscillate at different frequencies. Its effect on the waveforms is to be recorded.

Objective 4: **Construct and test the RF input and audio output stage.** In this stage, the output is disconnected from ground and connected to an output capacitor. This will then form an output to the audio amplifier. It is also optional to attach a second transistor to boost the AF output, and add a low pass filter before the AF stage to filter out any remaining carrier signal and quench. Once an aerial has been attached, it should be possible to receive and play radio signals. The main objective of this stage is to both observe the waveforms in the circuit and at its output using the oscilloscope and to attempt to tune to different radio stations.

Objective 5: **Simulate an external quench oscillator.** This stage deals with the use of an external quench oscillator. It was originally planned to construct a circuit which utilized a separate quench oscillator, however, time constraints did not allow this. As a result, it is intended to simulate an externally quenched SRR and then compare the results to those of the self-quenching design.

1.4 Project planning

The Gantt charts found in appendix A and appendix B show the allocation of tasks against the projected time frame. It also documents any amendments made in the project planning. As documented in section 1.3.2, the project is broken down into 5 different objectives.

Semester 1: The Gannt chart in appendix A demonstrates the time allocation for tasks in semester 1. The main changes to the plan made in this semester was abandoning the use of Multisim and MATLAB in favour of using LTSpice. The main objectives of the first semester were the 2 initial assessments. The research and simulation are ongoing processes for the duration of the project

Semester 2: In semester 2 the simulation stage was broken down into more specific tasks. The Gantt chart in appendix B shows the time allocation for various tasks. The original plan of building an externally quenched SRR abandoned in favour of simulating it. This is because serious over runs in the simulation stage, and the inability to get the simulation to work in time made constructing such a device unfeasible. The design and construction of the oscillator went to plan, however, a malfunctioning circuit caused time over runs on the SRR construction phase.

Chapter 2.0 – Theory and Background Research

2.1 Literature review

This section deals with the main publications and research material used in the background research for this project and how and where they were applied.

2.1.1 Super-regenerative receivers, J.R Whitehead (Whitehead, 1950).

J. R Whiteheads book was published in 1950, and is the most comprehensive document on the subject of super regenerative receivers. It explains the mathematical principles of super-regenerative theory as well as the principles of early valve based SRR design. This publication explains the principle of quench and details the waveforms appearance. It also discusses all of the circuit's parameters in all different modes of operation. Section 2.3 demonstrates some of the content from this publication which this project is going to attempt to prove.

2.1.2 FM Super-regenerative receiver, Burkhard Kainka (Kainka, 2007).

This web article documents the construction of an SRR in 3 simple stages. A large bulk of the fundamental design implemented in this project comes from this article. The procedure used in simulation and construction of the hardware constructed for this project follows the 3 steps outlined in the paper. This paper includes designs for receivers using both 1 and 2 transistors. Both of these designs were simulated, modified and constructed for this project, with varying degrees of success. This article also describes the method of testing to be used on an SRR and where in the circuit different waveforms will occur. These testing procedures were then applied to both simulation and hardware testing.

2.1.3 Designing Super-regenerative receivers, Dr Eddie Insam (Insam, 2002).

This web article, has a description of the mathematics involved in SRR theory as well as several different designs. The mathematics provided in this article is a summarised version of the mathematics included in (Whitehead, 1950), however, this article deals with transistor based SRR design, making its design content a more suitable reference to a project of this nature. Some of the designs included in this article bear similarity to those in (Kainka, 2007) but with some modifications and a greater degree of detail.

2.1.4 Transistor Super-regenerative Detection, Woo F. Chow (Chow, 1955).

This transcript from the Institute of Radio Engineers documents the results of the first tests into super regenerative detection utilising bi-polar junction transistors. The most important factor discussed in paper is the criterion of oscillation. This demonstrates the conditions under which the circuit will begin its distinctive quench oscillations. By taking this criterion of oscillation into account, observations can then be made on data acquired from simulations and tests and a comparison can be made between the predicted results taken from this paper, and the actual measured results from the tests. These results and comparison will form a large part of the discussion and conclusion of this project.

2.1.5 Super regenerative detector circuit usind transistors, Woo f. Chow (F, 1958)

This document is the patent for W F Chow's super-regenerative receiver using transistors. It contains the circuit diagram from which the designs for an externally quenched SRR are based.

2.2 The Theory of Radio Frequencies (RF)

RF is the use of electromagnetic radiation to communicate massages over long distances wirelessly. These beams of electromagnetic radiation are known as radio waves. At the source of a radio wave, a device known as a transmitter is required to produce and broadcast the radio wave. At the other end, a receiver is required to capture the broadcasted signal. Radio signals comprise of 2 signals, the carrier signal and the modulating signal (or messenger signal). The carrier signal is the frequency at which the message is broadcast, meanwhile the modulating signal is the message,

usually an audio signal, which the transmitter is broadcasting. Once the signals have been mixed together, the radio wave is said to be modulated. In the broadcast of analogue radio waves there are 2 main techniques of modulating a signal, Amplitude Modulation (AM) and Frequency Modulation (FM).These different methods of signal modulation will be discussed in sections 2.2.1 and 2.2.2 respectively. Once a modulated radio wave has been detected by the receiver, the message contained within the modulating signal must be separated from the carrier signal. This process is known as de-modulation. It is common practice for the modulating signal to be of a much lower frequency than the carrier signal.

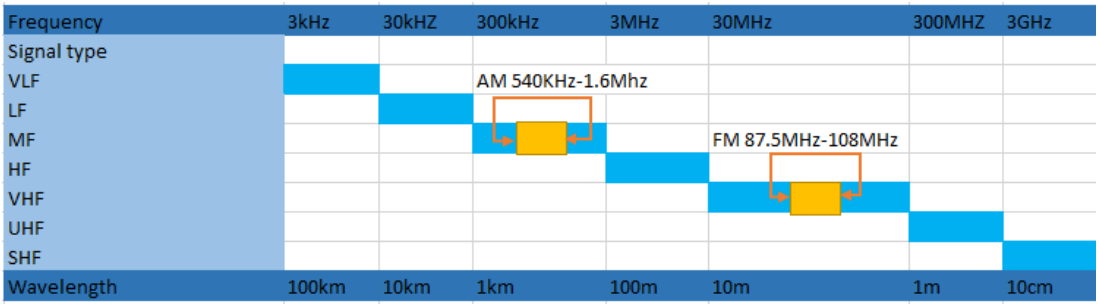

Figure 1 – Radio spectrum

Radio waves can be transmitted at different frequencies, typically between 3 kHz and 300GHz. The frequency at which the signal transmits is dictated by the frequency of the carrier signal. Different radio stations or different types of device utilizing RF, such as Radar use different frequencies. A radio receiving device can be tuned to receive a specific frequency, meanwhile blocking out all of the others. How a radio does this is one of the main themes of this project. Figure 1 shows the range of frequencies at which different radio bands operate. AM radio works in the 540 kHz to 1.64 MHz range, which is highlighted in yellow. It is visible from this chart that AM falls into the MW (Medium Wave) Bandwidth. FM works at much higher frequencies than AM. Typically the range of commercial FM stations is in the region of 87.5MHz to 108MHz. It is visible from the chart in Figure 1 that FM falls into the VHF band width. More specifically, FM's part of the radio spectrum is known as band II VHF. VHF covers an extremely large part of the spectrum, with frequencies ranging from 30-300MHz. As FM requires a larger amount of bandwidth to operate, it is placed in VHF as opposed to MW or HF as there is the available bandwidth for it to use.

2.2.1 Frequency Modulation Theory

FM radio stands for frequency modulation. It falls into a category known as angle modulation or exponential modulation. Angle modulation deals with both FM and PM (phase modulation) methods of transmission. Like AM, PM and a vast majority of other communication waveforms, FM signals consist of a carrier signal and a messenger signal. In the case of FM, the carrier signal is between 87.5-108MHz, which is in the upper end of the VHF scale, or Band II VHF as it is commonly known. The messenger signal is the input signal at the source of the radio broadcast, for instance, music or the voice of a radio DJ, possibly even a continuous wave form for generating Morse code. The Idea of the radio, as described earlier, is to break the incoming FM radio wave up in order to extract the messenger signal from the modulated signal.

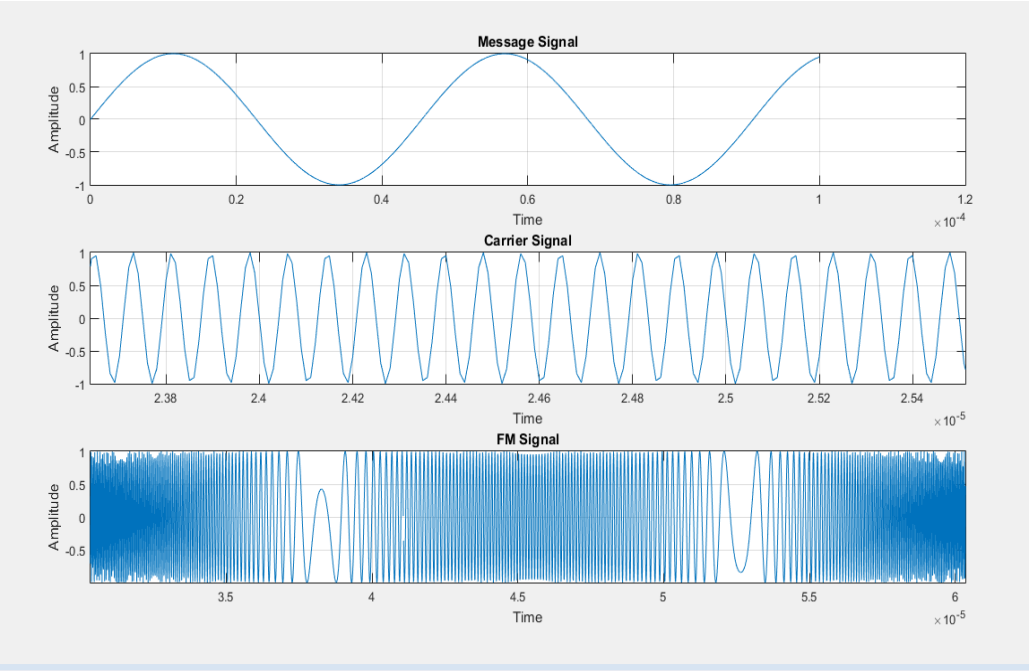

Figure 2 – FM wave components; carrier signal, message signal, combination

The basic principle of FM is that as the amplitude of the messenger signal modulates, the frequency of the FM signal modulates, hence the name frequency modulation. The intensity of these modulation changes is known as the modulation index. In the diagram above Figure 2, the FM signal is the one on the bottom. In the centre, the wave forms are less densely packed than on the left and right sides of it. This is where the frequency has modulated. With a low modulation index, this change in frequency

modulation would be less noticeable, but more prominent with a higher modulation index.

An FM wave can be expressed mathematically using the following equation:

$$\boldsymbol{V_{fm}(t) = V_c Cos[2\pi ft + \phi_c + 2\pi k_{fm} \int_{-\infty}^{t} V_m(t)dt]}$$

Here V_{fm} represents the magnitude of the FM signal in volts, V_c is the magnitude of the carrier signal in volts, magnitude of the modulating signal in volts, ϕ_c is the phase angle of the carrier signal, in radians or degrees, t is time, f is frequency and k_{fm} is the modulation index (sometimes represented as m instead).(www.circuitsgallery.com, Otung, 2001)

2.2.2 Amplitude Modulation Theory

The basic principle of the Amplitude modulated signal is that the modulating signal modulates the amplitude of the carrier signal. With an AM the modulation index dictates the depth at which the modulating signal modulates the carrier signal.

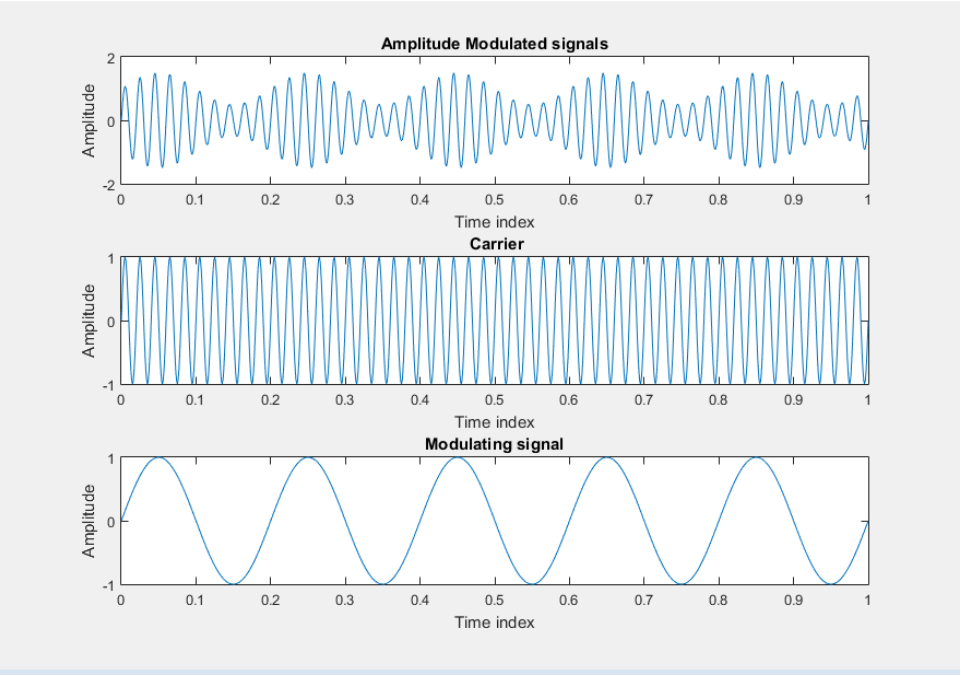

Figure 3 – Amplitude modulated wave form

Figure 3 demonstrates this principle. The waveform at the top shows an AM wave with a modulation index of 0.5. It oscillates at the same frequency as the carrier signal, displayed in the middle, meanwhile, its amplitude modulates at a frequency and magnitude relative to the modulating signal, displayed at the bottom. (Otung, 2001, www.circuitsgallery.com)

2.3 Theory of super regenerative radio receivers.

The super regenerative-receiver is a device which receives, amplifies and demodulates a radio signal. The SRR differs from other type of receivers in that it does the whole procedure with only one circuit containing a single transistor, whereas certain other types of radio receiver utilise individual circuits for signal reception amplification and demodulation.

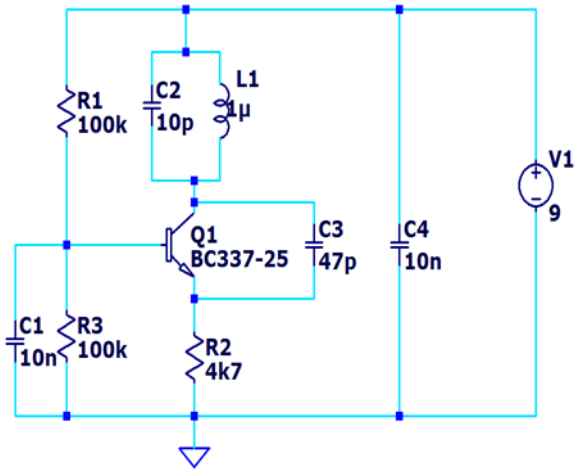

Figure 4-A tuned oscillator

2.3.1 The Oscillator

At the heart of a super regenerative radio is a simple oscillator. Figure 4 shows the schematic for one of these oscillators. This oscillator is based around the design from (Kainka, 2007). The oscillator consists of a tank circuit consisting of a variable capacitor and inductor in parallel (or shunt circuit as it is also known) and a transistor. A feedback capacitor is connected between the collector and emitter of the transistor. The resistors at the transistors base are responsible for bias.

This oscillator will produce a continuous sinusoidal signal. By modifying the value of L1 or C2, the frequency of this oscillation can be changed. The relation between the frequency and the value of these 2 components can be described with the following set of equations:

$$V = V_c + V_L$$

$$I = I_C + I_L$$

First, the entire voltage across the inductor and capacitor is equal to the voltage across the capacitor ($V_{c)}$ plus the voltage across the inductor(V_{l}). The same is true for the currents I_c and $I_{L.}$ The next thing to consider is the circuits reactance where X_c is the capacitive reactance, X_L Is the inductive reactance, F is the frequency in Hz, L is the inductance in Henries, C is the capacitance in Farads and ω is the angular frequency in radians per second:

$$X_c = X_L$$

And:

$$\omega = 2\pi f$$

Where:

$$X_c = \frac{1}{2\pi fC} = \frac{1}{\omega C}$$

And:

$$X_L = 2\pi fL = \omega L$$

Therefore:

$$\frac{1}{2\pi fC} = 2\pi fL \; and \; \frac{1}{\omega C} = \omega L$$

By further deriving this equation we can come to the conclusion that:

$$2\pi f^2 L = \frac{1}{2\pi C}$$

$$\therefore\ f^2 = \frac{1}{(2\pi)^2 LC}$$

And finally concludes that:

$$f = \frac{\sqrt{1}}{\sqrt{(2\pi)^2 Lc}} = \frac{1}{2\pi\sqrt{LC}} = \frac{\omega_0}{2\pi} \therefore \omega = 2\pi f = \frac{1}{\sqrt{LC}}$$

This manipulation of the oscillation frequency forms the basis of how the radio is tuned. By tuning this oscillator to the frequency of a radio waves carrier signal, the signal can then be detected.

2.3.2 Quench Oscillations

Fundamental to the operation of a super-regenerative receiver is the phenomenon known as quench Quench is the periodic gain and decay of the oscillations which build up in the oscillator. Super regenerative oscillators differ from standard tuned oscillators in that they produce quenched waveforms instead of continuous oscillations.

SRR designs fall into 2 categories, self-quenching and externally quenched circuits. Likewise, quench falls into 2 main different modes, linear mode and logarithmic mode. This project mainly deals with the effects of linear mode operation in a self-quenching circuit. **Error! Reference source not found.** shows different types of quench waveform. The waveform at the bottom (fig. 5.4) shows a linear quench waveforms from a self-quenching circuit.

The quench waveform is the one at the very bottom, while the saw tooth wave above it is what gives rise to the quench wave. The top 2 sets of waveforms 5.1 and 5.2) demonstrate that the shape of linear quench waves can be affected by the shape of the wave that gives rise to them. The top two waveforms are most likely created by an externally quenched circuit where the quench oscillator produces these waveforms. Finally, the waveform second from bottom (**Error! Reference source not found.**.3) is a logarithmic quench waveform.(Whitehead, 1950)

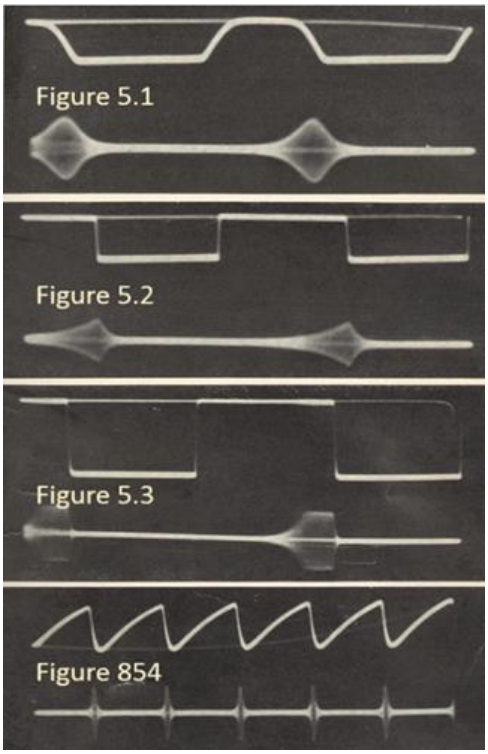

Figure 5-Quench waveforms(1950, Whitehead)

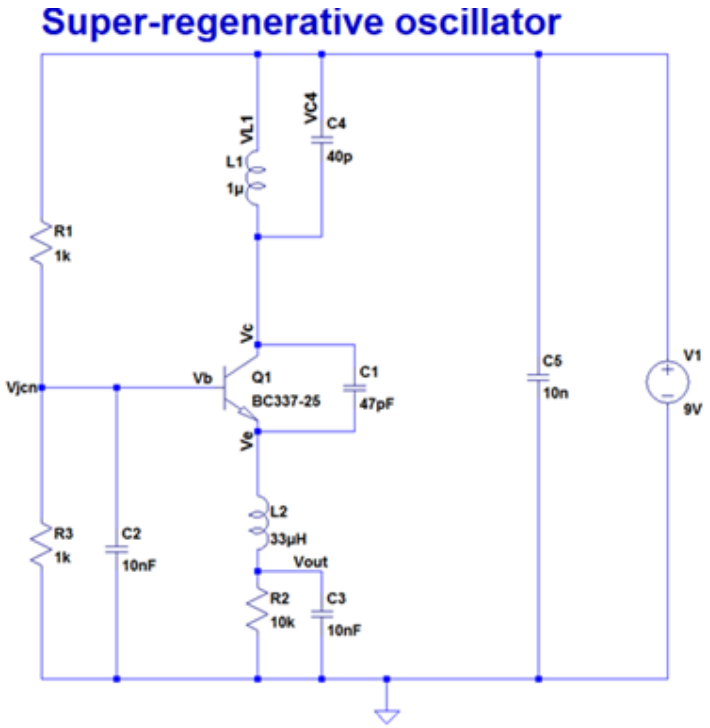

Figure 6-Super-regenerative oscillator

These quench waveforms demonstrated in Figure 5are from an SRR in its quiescent state. In an SRR, small amounts thermal noise can give rise to these oscillations. Likewise, a stimulus from an RF source can also give rise quench oscillations. The above schematic Figure 6shows the alterations which must be made to a tuned oscillator in order to turn it into a super regenerative oscillator (SRO).

Note the main difference between the circuit demonstrated in **Error! Reference source not found.** and the circuit in Figure 4is the inclusion of an adittional inductor, L2 and an additional capacitor, C3. The addition of these components fundamentally changes the behaviour of the circuit. The circuit demonstrated in Figure 6should give rise to the waveform demonstrated in Figure 5.4.

The quench waveform at the bottom should be found at the collector of the transistor, marked as Vc on the circuit diagram, meanwhile the sawtooth wave should be found at the point Vout, marked on the circuit diagram underneath the inductor L2. There are several factors which affect how this happens. Fundamental to this is a phoenomenon known as time varying conductance. The circuit in (Figure 7) shows the equivalent circuit of the shunt part of the oscillator.

While the actual oscillator its self only contains the the inductor and capacitor as physical componrnts, the parasitic resistance of the inductor must be acounted for. More importantly, the parallell conductance, represented as G on the diagram becomes a key factor in the operation of this circuit. Conductance is essentially the opposite of resistance. Conductance can be represented as 1/R and can be assumed to be relative to the total resistance in the system. The current source I1 is the stimulus which initiates the oscillations, coming from either an RF source or thermal noise in the system. Here, I1=i(t)=Asin(ωt) where ω=1/√LC. The resulting current in the circuit can be solved using the following differential equation:

$$C\frac{dV}{dt} + G(t)V + \frac{1}{L}\int V\,dt = Asin(\omega t)$$

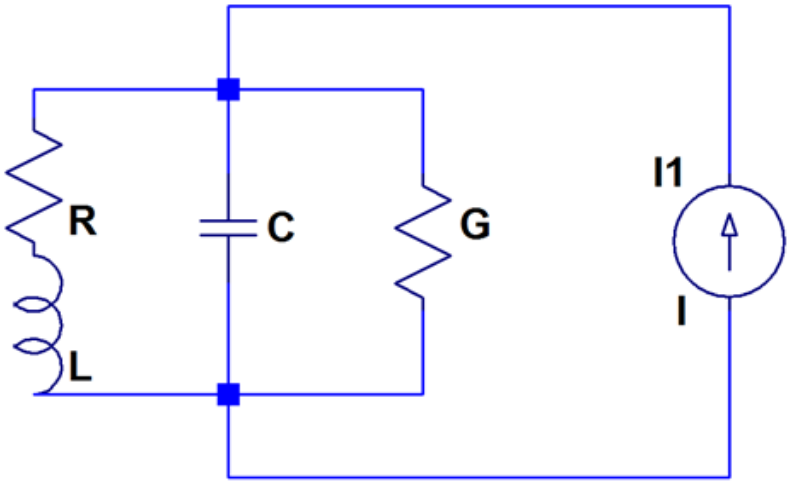

Figure 7 – Shunt circuit

The assumption made here is that the value of the conductance, G is constant, and as a result the amplitude and frequency of the output, Asin(ωt) is also constant. The reality, however, is that G does not remain constant (hence time varying conductance). The diagram below taken from (1955, Chow) graphically represents what is known as the criterion of oscillation. It demonstrates that as the current at the emitter, I_e and the collector voltage, V_c fluctuate, they create oscillations as both I_e and V_c enter the oscillation region.

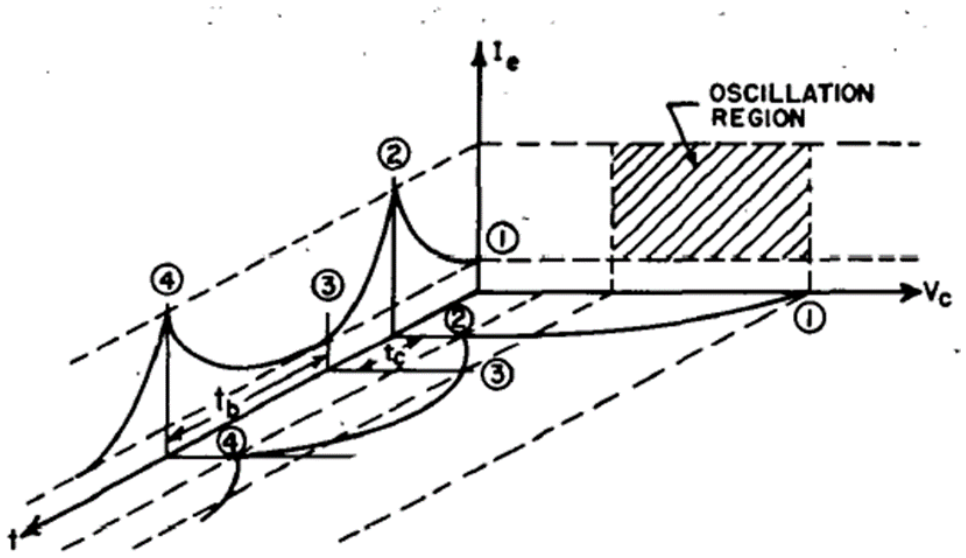

Figure 8 –graphic representation of the criterion of oscillation (1955, Chow)

The oscillations occur when the currents and voltages are at levels where an appropriate bias point is created. This is represented in Figure 8 by the shaded area

titled oscillation region. Figure 8 demonstrates the conditions required to bias the transistor in such a way that its gain is adequate to produce the quench. The different points marked on the time axis (t) represent different points in the quench cycle.

1. At point 1, t=0 and the initial values of V and I are displayed.
2. At point 2 both I and V are out of the oscillation region. The oscillation ceases. As V starts to rise again, it heads towards point 3.
3. Once the V crosses over the dotted line representing the lower limit of the oscillation region, the oscillations start to build up again. They continue to build up until V hits its peak. As V starts to decrease again, the oscillation will begin to decay, until it crosses the dotted line again, at which point it will completely cease.
4. At point 4, it is in the same state as in point 2 and the process will repeat.

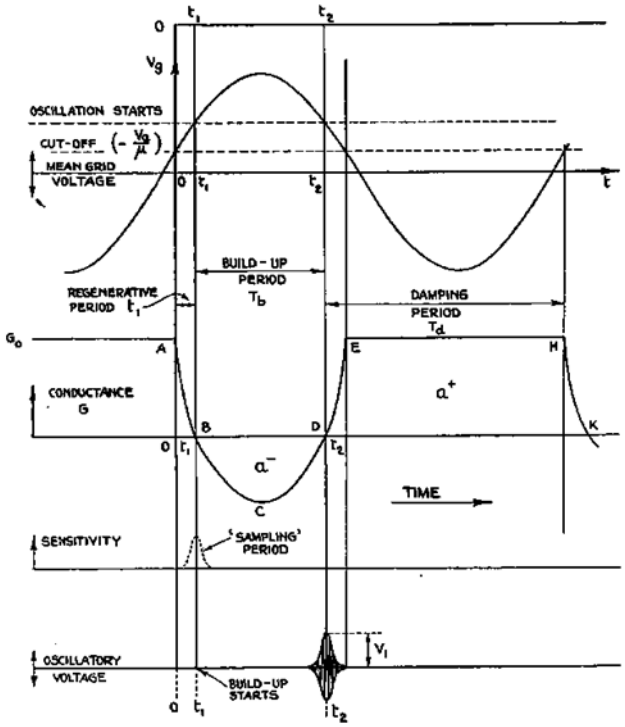

Figure 9 – Grid voltage, conductance cycle and oscillatory voltage (1950, Whitehead)

The conductance of the transistor will also fluctuate with this change in voltage and current. This is because the trans-conductance, gm, of a transistor is proportional to its collector voltage and emitter current and can be defined by the following equation:

$$g_m = \frac{\Delta i_{in}}{\Delta V_{out}} = \frac{i_c}{V_{be}}$$

When the value of G=0, the transistor is effectively switched off. Figure 9 from (1950, Whitehead) demonstrates an alternative to Chow's model in Figure 8. In this figure, the criterion of oscillation is described by the interaction between the conductance, G, and the grid voltage, V_g. While this model is based around older versions of SRR design, using thermionic valves, the grid voltage is equivalent to the voltage between the base and the emitter of a BJT (V_{be}). The SRR can only detect radio frequencies when the quench is active. This effectively makes the quench operate like a sampler. The higher the frequency of the quench, the higher the fidelity of the received signal. If the frequency of the quench is too high, however, then it will ceace to quench and the oscillations will revert back to their continious state. Quench frequencies can also be modulated by RF frequencies. If the quench is already at quite a high frequency, having its frequency modulated further can cause the quench to ceace. As a result, quench frequency needs to be controllable to compensate for this. Figure 9 demonstrates a sinusoidal voltage giving rise to the quench oscillation. This is known as the slope controlled state. For sinusoidal and sawtooth shaped waveforms, where the waves amplitude increaces in a slope, these waveforms will always fall into the slope controlled category.

2.3.3 Externally quenched circuits and different quench waveforms.

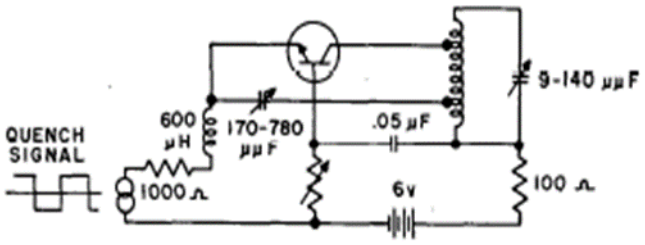

Figure 10 – An externally quenched circuit (1955, Chow)

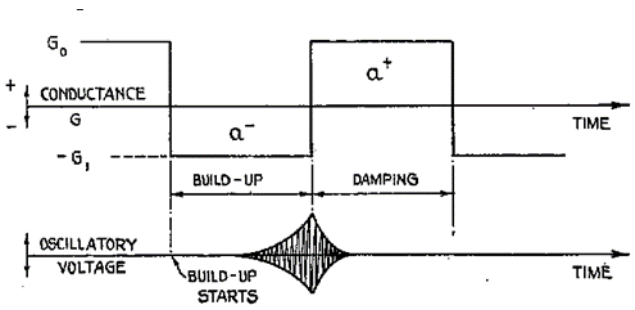

Figure 11 – Conductance and quench cycle of a step controlled square wave quench oscillation (1950, Whitehead)

It is demonstrated in **Error! Reference source not found.**.4 that when operating in self-quenching mode, a saw tooth waveform will be produced. This saw-toothed voltage will in turn follow a saw toothed conductance cycle. If the quench cycle is to be controlled by a different shaped wave, however, then it is necessary to produce this wave using an oscillator specifically designed to produce the desired shape of waveform. Figure 10, taken from 1955, Chow, shows a circuit where an external quench signal is introduced. This signal is represented by a current source, rather than circuit diagram of an actual oscillator. In this case, it is producing a square wave quench signal. If, the quench signal was sinusoidal or saw tooth, this circuit could be said to be operating in slope controlled mode as described in section 2.3.2, however, in the case of a square wave, where the wave changes from its lower peak voltage to its higher peak voltage almost instantaneously as opposed to in a gradual slope, as is the case in slope controlled mode, then the circuit can be said to be operating in step controlled mode instead. Having an external quench oscillator is essential to allowing the SRR to operate in step controlled or logarithmic mode. Figure 11 shows the conductance cycle and build up and decay of a step controlled square wave quench. This is the kind of conditions which would occur in the circuit demonstrated in Figure 10

Chapter 3.0 – Design, Simulation and Construction Procedure

The design of the super-regenerative receiver was done in several stages. The first stage was to design and simulate the circuit in 3 stages. The results of the simulations provided a good insight as to what was happening inside the circuit and weather the circuit under construction was a feasible design to actually construct. Once simulations had been run and the results were satisfactory, they were then constructed and tested. The simulation was schematic was designed and tested in 4 stages:

1. Design and simulate an oscillator circuit capable of oscillating in the band II VHF region of frequencies.
2. Design and simulate a super-regenerative oscillator capable of producing quench waveforms.
3. Design and simulate the finished super-regenerative radio receiver capable of producing an audio output.
4. Design and simulate an SRR with an external quench oscillator.

The first 3 stages of the design were based around the designs from (2007, Kainka). This article gave insight into a very simple, step by step method of designing, simulating and constructing an SRR.

The design provided on (2007, Kainka) did, however, have one fundamental flaw. Kainka's schematic involved the use of a BC494 transistor, a model which is not easily available, and has no available spice model, making simulating it impossible without writing a complicated net list based on the transistors properties. This meant an alternative model of transistor had to be found. Kainka's design suggested the use of a specialist RF transistor, capable of operating at high frequencies and producing adequate gain. The eventual transistor of choice was the BC337-25. This transistor was chosen due to its easy availability and the opportunity to simulate it on LT spice without the need to import a net list model for it. Another variation of this design, courtesy of Dr Simon Busbridge implemented a BC547 for this purpose, however, in (2007, Kainka) it strictly states that getting optimum results using this type of transistor is difficult.

The first major modification of the design in (2007, Kainka) was to change the values of the resistors at the base of the transistor. The BC337-25 has completely different parameters from the BC547 and BC494, and as a result it would require different values of resistance at its base so as to ensure the correct current at the base to allow the circuit to function properly. An initial test was done on the transistors to determine differences in their curves. It was from these observations that the value of the resistors required could be estimated, before being tested in a simulation. The 2 charts in appendix C and appendix D show the BJT parameter curves plotting the voltage across the collector and emmitter against the collector current at different base currents.

The circuit diagram in appendix E was used to simulate the BJT parameters in appendices C and D. They were created on LT spice. The results were then expored to MS excel. It works by applying a step current to the base of the transistor and a gradually increasing pulse voltage across the collector and emitter. Voltage readings were then taken from the node CE, and current readings from the base and collector in order to produce the charts.

3.1 Oscillator design, simulation and construction

3.1.1 Design and simulation

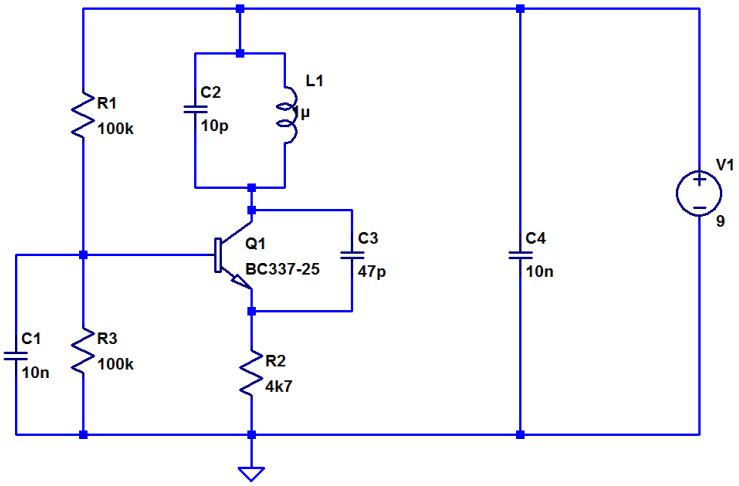

Figure 12 – Tuned oscillator

The objective of this simulation was to design, simulate and then construct a circuit capable of producing oscillations over a wide range of frequencies .The schematic in Figure 12 shows the layout of this circuit, produced using LTSpice.

Fundamental to the function of this circuit was the choice of values for the capacitor and inductor in the tank circuit. As described in section 2.2, the values of these components are what dictates the frequency the circuit will oscillate at. The graph in figure 14 shows the frequency the circuit will oscillate at with different values of

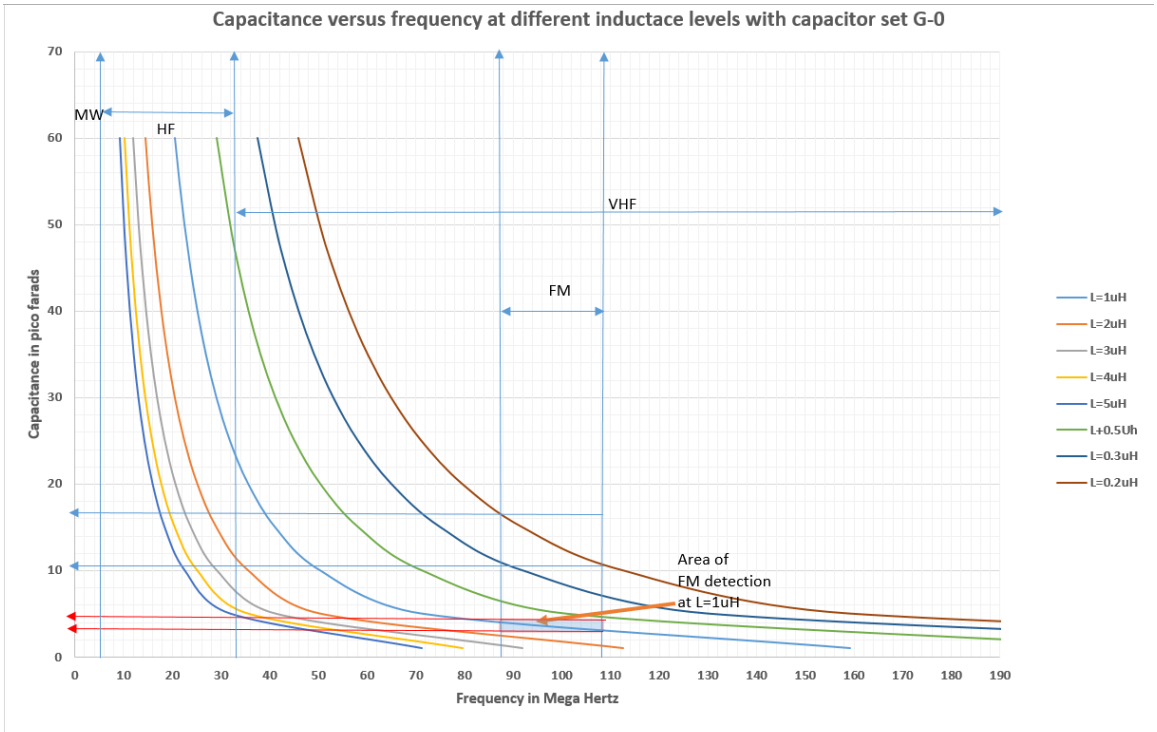

Figure 13 – Frequency vs capacitance G-O

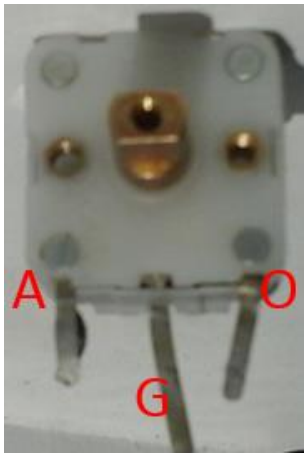

Figure 14 – A Varicap and its teminals

capacitance and inductance. In the simulation, a standard capacitor was used and its value was changed in every subsequent test to emulate the effect of a variable capacitor. This was done as the LTSpice component library does not contain a model of a variable capacitor, and one could not be created without some complicated manipulation of LTSpices net list writer. The variable capacitor used was a TTWM 2 gang variable capacitor. The phrase 2 gang means it is effectively 2 variable capacitors in one unit. The device has 3 terminals, named A, O and G. Wiring up the device between terminals O and G gives a range of capacitances between approximately 0-59.2 pico farads, while between A and G the range is approximately 0-141.6. It was proposed that the inductor would have a set value, because variable inductors are elaborate devices which could

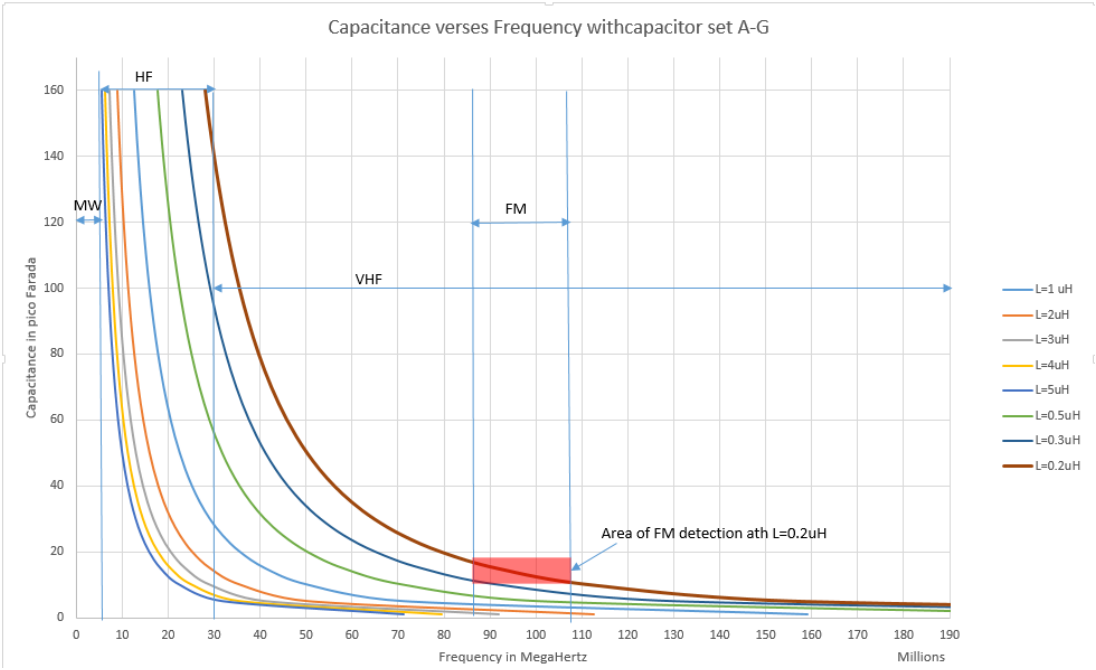

Figure 15 – Frequency vs capacitance A-G

possibly over complicate the design. The circuit, was, however, simulated using different values of inductance to help get an idea of which value inductor could give an optimized performance. The charts above show the frequencies the circuit is supposed to oscillate at with different values of capacitance and inductance. The chart in figure 16 shows the capacitance vs frequency of the varicap wired between G and A. From these charts it is possible to conclude, that while G-A allows a larger amount

of the frequency spectrum to be tuned into, it also makes the receiver less sensitive. Looking atFigure 15, it is possible to see that the entire FM bandwidth can be tuned into over a change of only 2 or 3 pico farads. This means only the slightest movment on the varicap could cause a cahnge in frequency of tens of MHz, making precision tuning to a specific frequency very difficult. Wiring the varicap from O-G however, will decreace this sensitivity, making tuning easier, but at the sacrifice of bandwith which can be tumed to. Another factor in reducing the sensitivity of tuning is the inductance. Larger inductors make the maximum tunable frequenct smaller and the amount of change in capacitance needed to drastically alter the frequency much smaller. Using a smaller inductor, on the other hand makes the ratio of change between capacitance and frquency much smaller, allowing for more precise tuning. From these calculations, it was decided to use the varicap wired up between O-G for optimum results, as opposed to A-G although the circuit was designed to make changing between the two options simple. An inductor of 1µH was used, despite the fact that a smaller inductor would have been better, high precision 1µH inductors are available from Wurth Elektronik which would alow for more precise measurements to be made during testing. Please see appendix J for a full table of figures used to create this chart.

3.1.2 Construction of the oscillator.

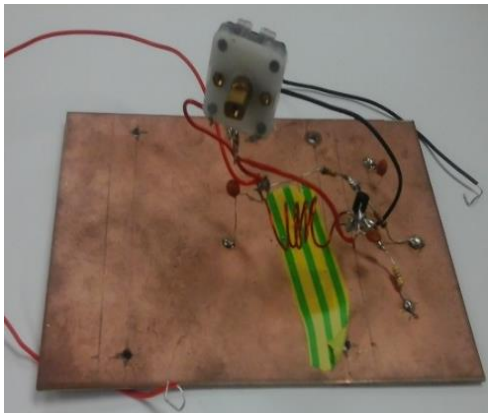

Figure 16 – Simple oscillator

2 oscillators were constructed for this project. The first oscillator was constructed using the ‘ugly build’ tecnique. It was constructed onto copper plated board and all connections were made by soldering togeather the terminal leads of the components. The circuit was grounded by soldering the grounded connections to the copper plated board, which was in turn connected to the –Ive o/p of a 9vDC source. The design for this oscillator came directly from (2007, Kainka), with the only change made to the design being the use of a BC337-25 transistor instead of the BF494 and the use of 100kΩ resistors instead of 10kΩ. The aim of constructing this oscillator was to have a test unit which

gave an idea of how this device would operate. The second oscillator to be constructed was actually incorporeted into thefinal SRR design.

The idea was to use jumpers that could disconnect the emitter from R2 (see figure 23) then use another jumper to connect the emitter into a second inductor and capacitor which forms the SRO. The purpose of this was to be able to isolate the oscillator and use it to calibrate the frequency the SRR is supposed to receive at. The image in Figure 16 shows the completed 'ugly build' oscillator.

3.2 Design, simulation and construction of a super-regenerative oscillator.

3.2.1 Design and simulation

This stage of the design process was the most challenging. While the appearance of the SRO is very similar to that of the standard tuned oscillator, its behaviour is radically different.

The addition of an inductor and additional capacitor coming from the emitter of the transistor is what causes the periodic gain and decay of the oscillations known as quench. The conditions under which the circuit would behave this way were difficult to create, as the slightest variation of value on any single component in the circuit could either cause the quench to stop and revert back to its continuously oscillation state, or stop oscillating all together. It was in this stage of the design process where the modifications made to the original design from (2007, Kainka) were most significant. The schematic Figure 17 shows the circuit implemented at this stage of the design process. The objective of the tests on this circuit was to observe the changes in current and voltage at all different nodes and components in the circuit, and to see how changing the values of some components would change these currents and voltages. One very distinct feature of LT spice is that by default, it assumes that all inductors

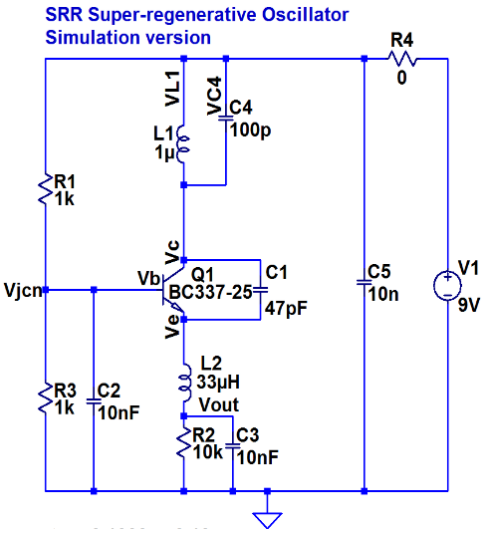

Figure 17 – Super regenerative oscillator schematic

and capacitors are ideal, and thus, have no losses or series/parallel resistance. This can prove problematic as without these losses and series resistance the circuit would not quench due to the tank circuit's Q factor being infinite. This has 2 possible explanations. Q factor is calculated by frequency × (energy stored/ average power dissipated). If the program assumes ideal conditions, then no energy will be dissipated, hence the equation for Q factor would become:

$$Q = \omega \frac{energy\ stored}{avg\ power\ dissapated}$$

$$= \omega \frac{energy\ stored}{0}$$

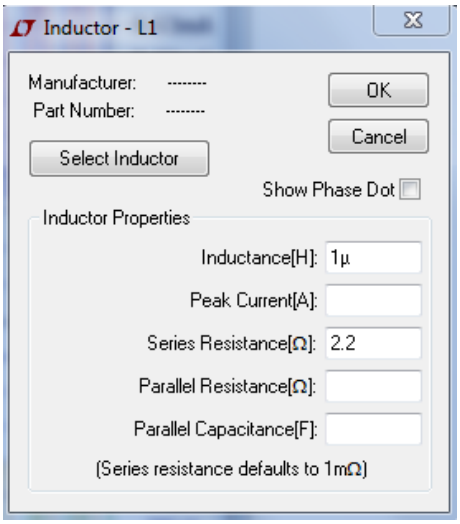

Figure 18 – Series resistance setting in LTSpice

It is widely regarded among mathematicians that division by zero is an impossibility, with some arguing that it would equal infinity and others just calling it a folly with no real definition. Suppose the program LTSpice assumes the answer to equal infinity or zero, then that would mean the Q factor would be infinite or zero. Since quench is based around varying conductance in a circuit, then when the conductance reaches a lower level or a negative amount, then there will be increased resistance and a constantly changing level of power dissipation, which in turn can be made into an average power dissipation. Simply put, quench cannot happen without a Q factor, Q factor cannot happen without power dissipated, and power dissipation cannot happen without some kind of resistive element. There are 2 solutions available to this problem. First of all, the inductor L1 could be simulated with a resistor of negligible value in series with it, or as Figure 18demonstrates, it can be manually programmed to have a series resistance.

3.2.2 Construction of the super-regenerative oscillator (SRO)

The construction of the super regenerative oscillator is one of the most fundamental stages of this project, for it is from this stage that a large amount of the raw data was

acquired. The circuit was constructed on perf-board and used the ugly build method, where all connections between components are made either through connecting the terminals of components together or connecting them with wires. The advantage of this construction method is that it eliminates parasitic capacitance which can occur in Vero board, breadboard and etched circuits. This parasitic capacitance can seriously hamper the performance of RF circuits. The final schematic (figure 23) includes the SRO. A series of jumpers allows certain parts of the circuit to be isolated. By removing the jumpers X12, X17 and X 19 then placing in the jumpers X13 and X18, the circuit will function purely as a SRO.

3.3 Design, Simulation and Construction of the Super-regenerative receiver

3.3.1 Design and simulation

The transition from super-regenerative oscillator to super regenerative receiver is a simple one. Figure 19 shows basically the same circuit as shown in Figure 17, but with C3 going to a simple audio output. The resistor R5 is there to simulate the load of a 400Ω set of headphones. An audio output of either 400Ω or 320Ω was suggested in (2007, Kainka) was put in its place. A1 is an attempt at simulating an RF input. This produces an AM input.

3.3.2 Finalised design and construction

The schematic (Figure 23) on page 39 shows the final design in great detail. The circuit was constructed in 4 stages. Each of these stages could be isolated from one another by a number of jumpers, then tested individually.

Stage 1, Oscillator: The first stage to be constructed was the oscillator. This consists of the inductor L1, the variable capacitor VC1, the transistor Q1 and the resistors R1, R2 and R3 and the capacitors C1 and C2. R2 is connected to the emitter of Q1 via the jumper X12. When the oscillator is configured, all other jumpers are removed.

Stage2, SRO: By removing the jumper X12 and then connecting the Jumpers X13 and X18, the circuit then behaves the same as the SRO circuit described in Figure 17. X13

diverts the current to go through L2, VR1 and C3 while X 18 pulls the current through C3 to ground.

Stage 3, SRR, simple output: By removing the jumper X18, then connecting the jumpers X19 and X15 and connecting the aerial to a small connector at the base of Q1, the circuit becomes a receiver, capable of picking up RF signals and demodulating them.X19 connects the output to go from C3 into C6 and X 15 connects C6 to the output, O/P 1. This O/P consists of a 3.5mm jack, which can then be connected to 1W stereo amplifier via a 3.5mm stereo cable. The output does not operate in true stereo, due to the fact that the signal applied to the tip and the ring both come from the same source, however, a signal is applied to both the tip and ring of the connector so as to ensure that a signal goes into both of the 2 channels in the stereo amplifier. The stereo amplifier used is a pre-built Mindsets 1W stereo amplifier.

Stage 4, SRR with low pass filter and pre-amp: This stage is an advancement on the previous stage, and aimed to solve some of the problems of low sound quality encountered when the circuit is set up as described in the previous stage. By removing jumper X 15, and connecting jumpers X 14 and X17, the signal coming from C6 then becomes connected to the low pass filter and pre-amp. The aim of this stage is to boost the signal going into the output, O/P 2 and to attempt to filter out any of the remaining quench, which causes crackling and distortion. The filter was designed to filter out between 41-50 kHz. This is the frequency that the quench is most effective at. The filter was constructed from a 1K variable resistor and 3.9nF capacitor. Altering the value of the variable resistor between 1kΩ and 0.8kΩ will allow it to filter 41-50 KHz. The following equation demonstrates how the filter was calculated:

$$f = \frac{1}{2\pi RC} = \frac{1}{2\pi(1 \times 10^3) \times (3.9 \times 10\text{^} - 9)} = 40808.955Hz$$

Where f is the cut-off frequency, R is resistance in Ohms and c is capacitance in nano-farads.

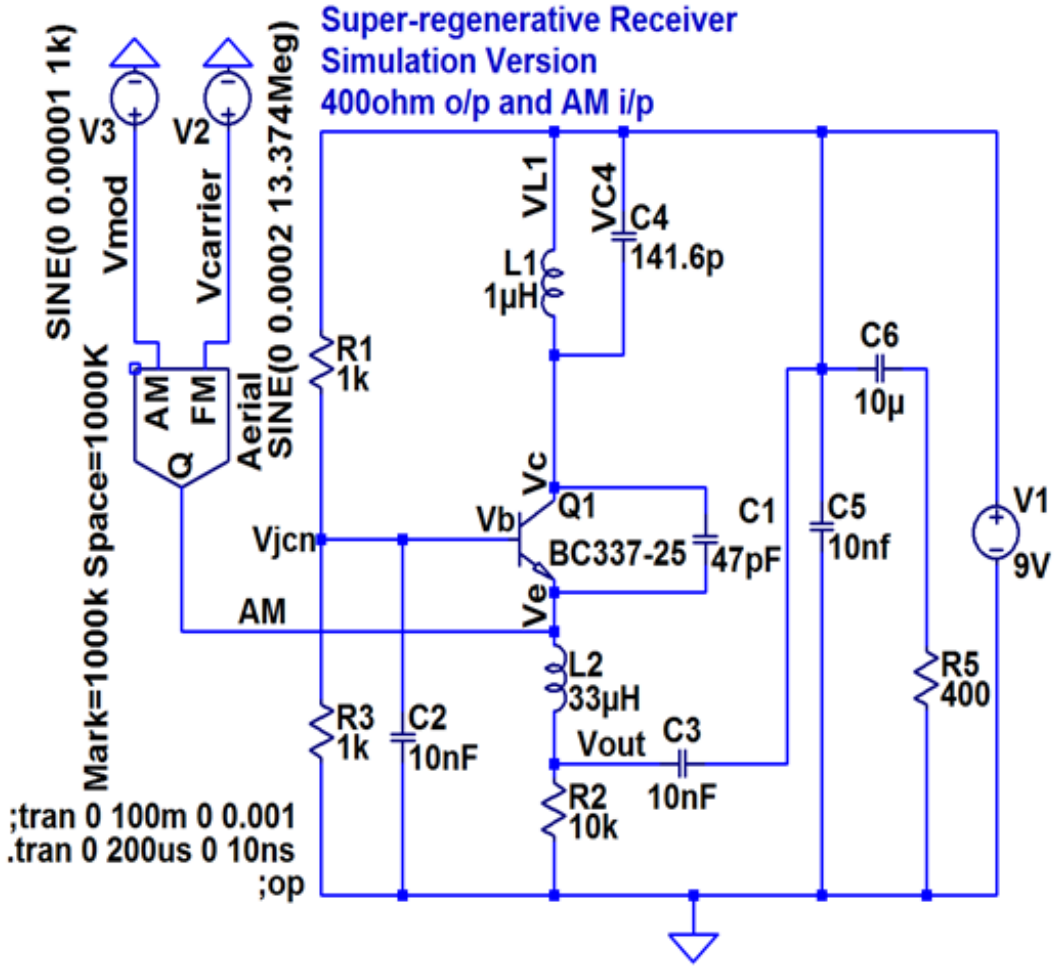

Figure 19– Super regenerative receiver with simulated RF input.

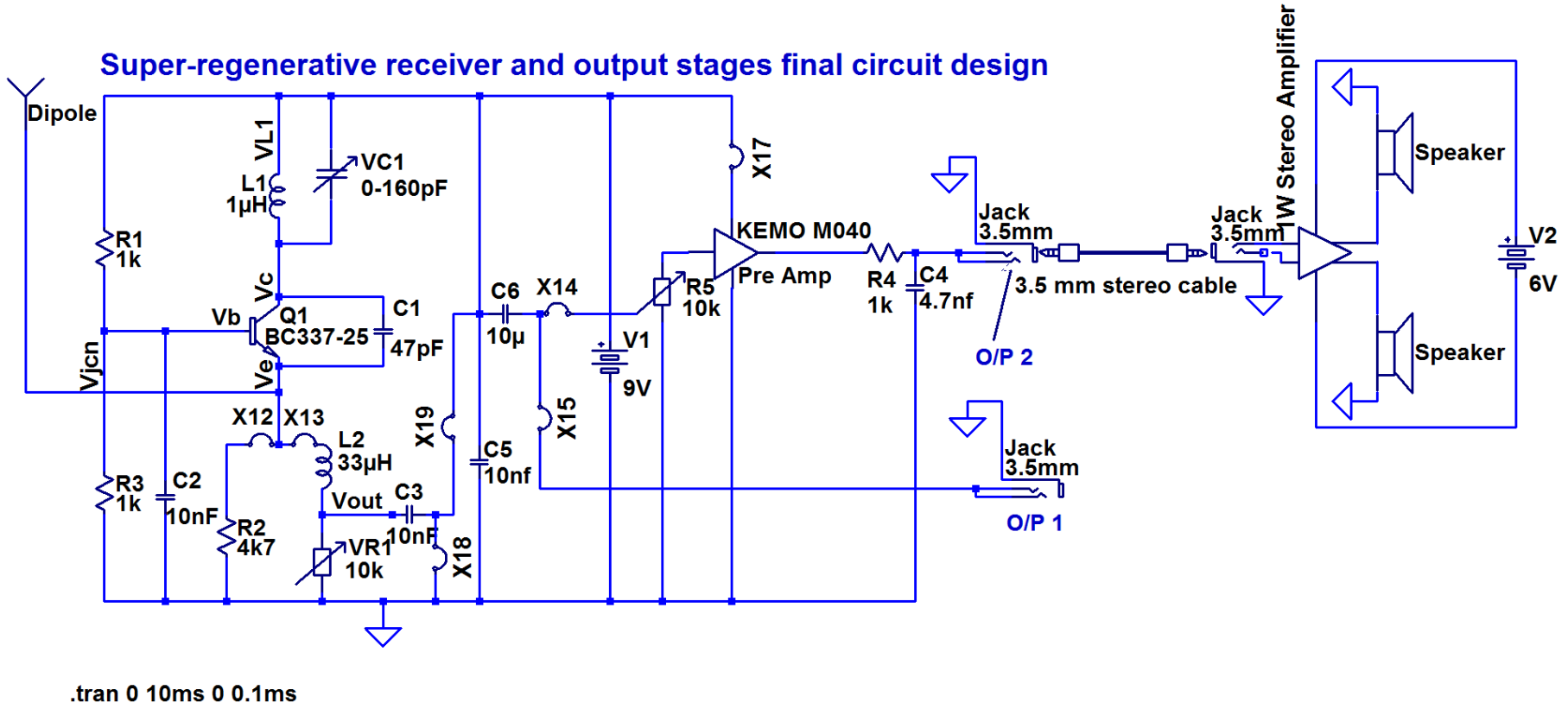

Figure 20 – Schematic of final SRR circuit and amplification system.

3.4 Externally quenched SRR

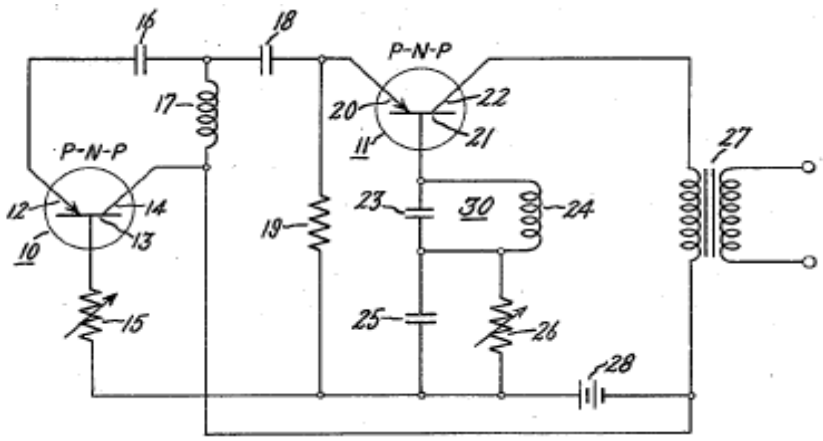

Figure 21 – W. F. chows original externally quenched SRR design (F, 1958)

This section deals with the design and simulation of an externally quenched SRR. Unlike the self-quenching SRR, the externally quenched SRR relies on a separate oscillator to create the quench. This simulation was based around a design by Woo F Chow. Figure 21shows the circuit which W.F Chow had patented in 1955. This is one of the very first designs of externally quenched transistor based SRR. The first design took the template of Chow's design and replaced it with component values used in the self-quenching version (Figure 22). This experiment, however, didn't succeed. As a result, a new experiment was attempted by taking the existing self-quenching SRR and

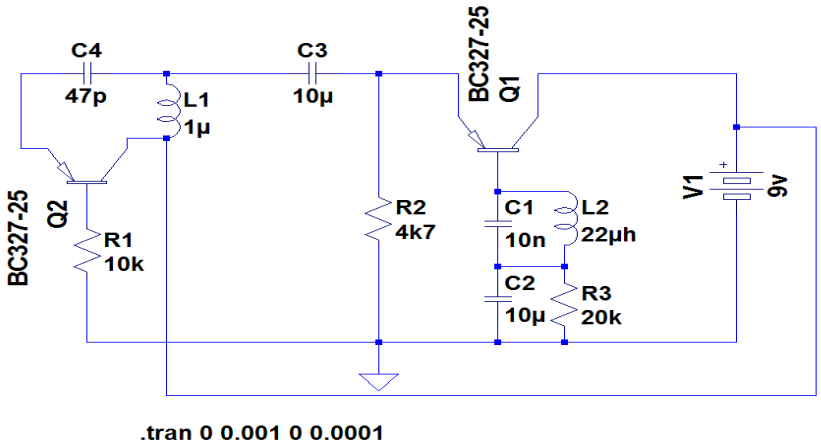

Figure 22 – Attempted simulation of W.F chow's design.

putting a voltage or current source going into the emitter of the transistor. While this experiment did not result in a successful design, it served as a useful test bench to further develop a working externally quenched circuit. Figure 23 shows the circuit with the voltage, V2 acting as an external quench. V2 could also be replaced with a

current source, I1 and experiments could be made attempting to control the quench by using a current source instead of a voltage. The design in Figure 24 shows another, earlier unsuccessful attempt at using a Colpitts oscillator as an external quench. Using the data acquired from Figure 23 could be used to further advance this design.

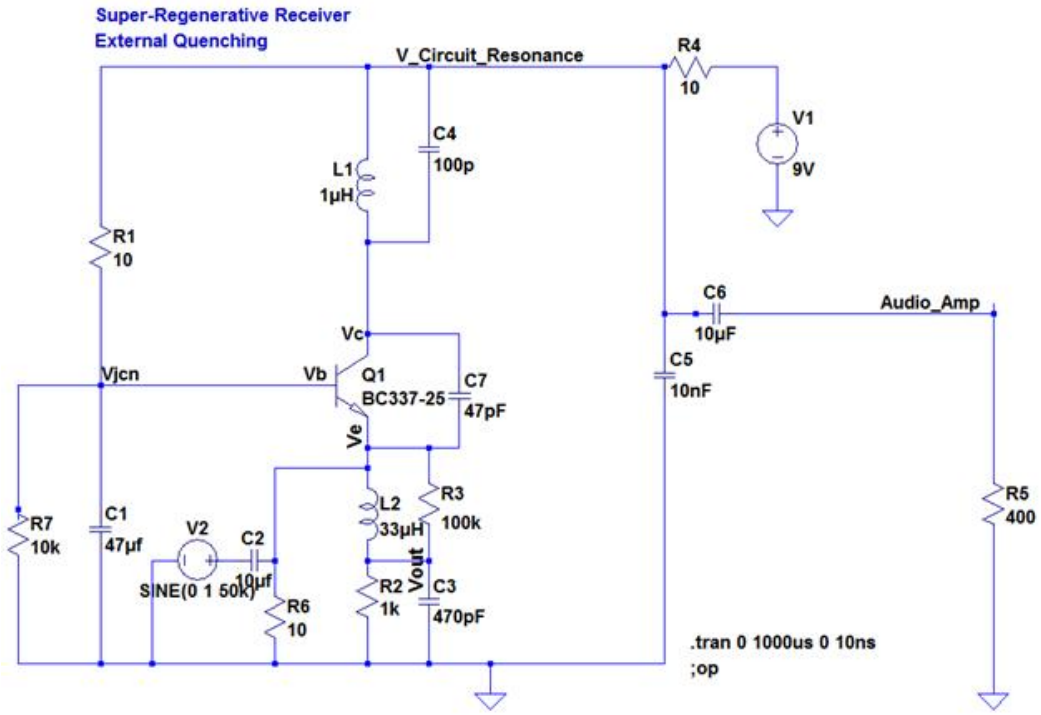

Figure 23 – SRR using voltage or current source as an external quench oscillator

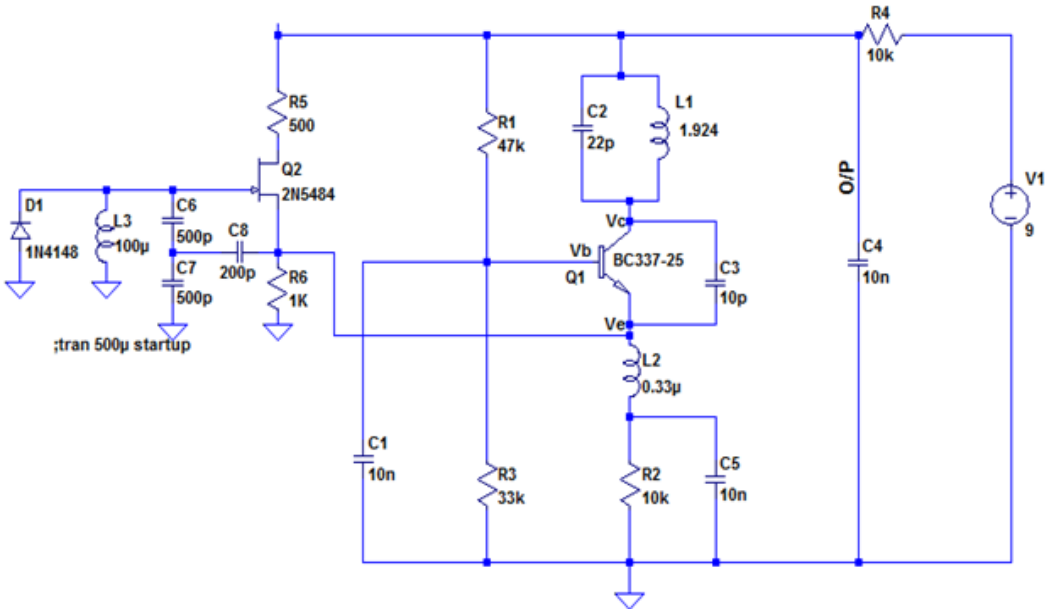

Figure 24 – SRR using Colpitts as an external quench oscillator

Chapter 4.0 Results and Discussion

This section is broken down into 3 parts. Fist, the predicted results for the tests are investigated. The second part deals with simulation results of the tuned oscillator, SRO and SRR. The third part deals with the test results from the final circuit tested at different stages of construction.

4.1 Predicted results

4.1.1 Oscillator

The prediction for the oscillator is that the frequency should be affected by changing the value of the variable capacitor. Frequency should change as the capacitance is changed from 1-160pF. This is based against using a 1µH inductor. This prediction was based on the following equation, using C as a variable and L as a constant:

$$f = \frac{1}{2\pi\sqrt{LC}}$$

The prediction is that the actual recorded results will show the same pattern as the one displayed in Figure 15.

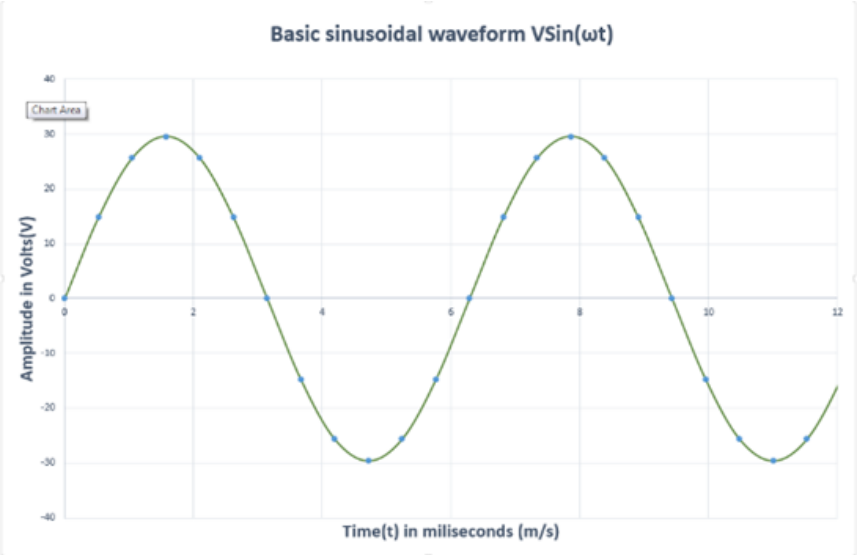

Figure 25 – Basic sinusoidal wave form

Figure 13For instance, if the capacitance is 10 pF, the oscillator frequency should be 50MHz. The output of the oscillator should be sinusoidal in shape, as demonstrated by the waveform in Figure 25.

4.1.2 Super regenerative oscillator, predicted results.

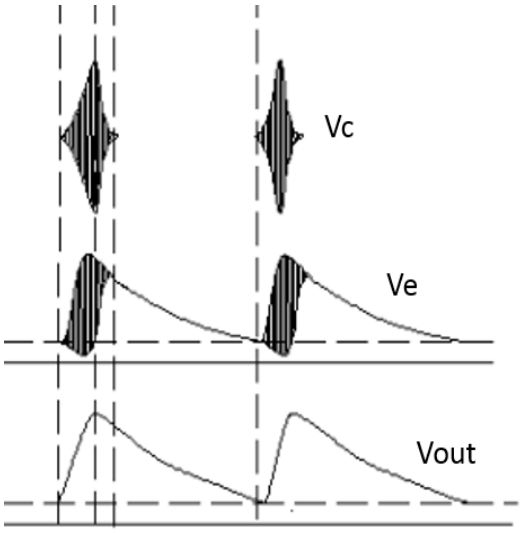

Figure 27 – Predicted waveforms at Vc, Ve and Vout (2007, Insam)

The results predicted for this stage are based around the behaviour of the super regenerative oscillator described in (1950, Whitehead) and (2007, Insam). **Error! Reference source not found.** in section 2.3.2, from (1950, Whitehead) demonstrated the basic appearance of different types of quench waveform. (2007, Insam) describes where in the circuit each of these waveforms is to be recorded from. The image in Figure 27 taken from (2007, Insam) shows the waveforms and the nodes on the circuit from which they should be recorded. Figure 31 shows the super regenerative oscillator schematic with the relevant nodes marked from where the measurements should be taken. As figure 30 shows, the distinctive quench waveform is the collector voltage, and can be found between the collector of the NPN transistor and the tuned oscillator, consisting of L1 and C4. The waveform coming from the emitter, Ve is shown in the middle of fFigure 26 and can be measured between the emitter and the inductor L2. The bottom waveform, Vout should be viewable from the net marked Vout on the Figure 26, at the node between R2, C3 and L2.

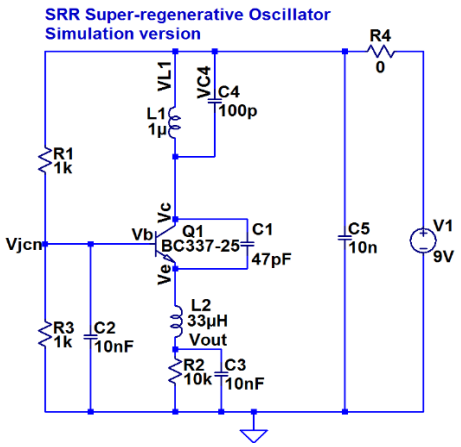

Figure 26-SRO

The main objective of this stage is to observe the waveforms from both the simulations and the final constructed circuit and observe any similarities between the predicted results and actual recorded results.

The waveforms in Figure 27 are based around measurments taken from a circuit featured in (2007,Insam). Like the circuit fetured in Figure 26, it was a self quenching circuit with a very large similarity to the circuits analysed in this project. It is therefore reasonable to make an assumption that the waveforms demonstrated in Figure 27 are a good predictive model on which to base any observations.

4.1.3 Super-regenerative receiver, predicted results

It is stated in (1950, Whitehead), that under stimulus from an RF source, several changes will occur in the appearance and behaviour of the quench waveforms. This is dependent on 2 main factors, the frequency of the incoming signal, and the type of signal. Figure 28, taken from (1950, Whitehead) shows the pattern the output from a super-regenerative receiver should take, dependant on the type signal applied to the receiver and the type of quench used in the receiver. Waveform (a), shown at the top is the modulating signal, which is the element of the RF which the SRR is trying to demodulate from the carrier signal. Waveform (b) shows a linear mode quench with its amplitude affected by the modulating signal. It is assumed that this could be the result of an amplitude modulated signal on the receiver. In this waveform, the spacing of the quenches remains constant. Waveform (c) demonstrates the behaviour of the output in logarithmic mode. The spacing of the middle point quenches remains constant, however, their width and duration of the quenches varies relative to the cycle of the modulating signal. While this project is not too concerned with the logarithmic mode, it is worth noting the correlation between the thickness if the quench lines in (c) and the spacing if the lines in (d). Waveform (d) is the predicted output for a self-quenching SRR. Here, the spacing of the quench lines

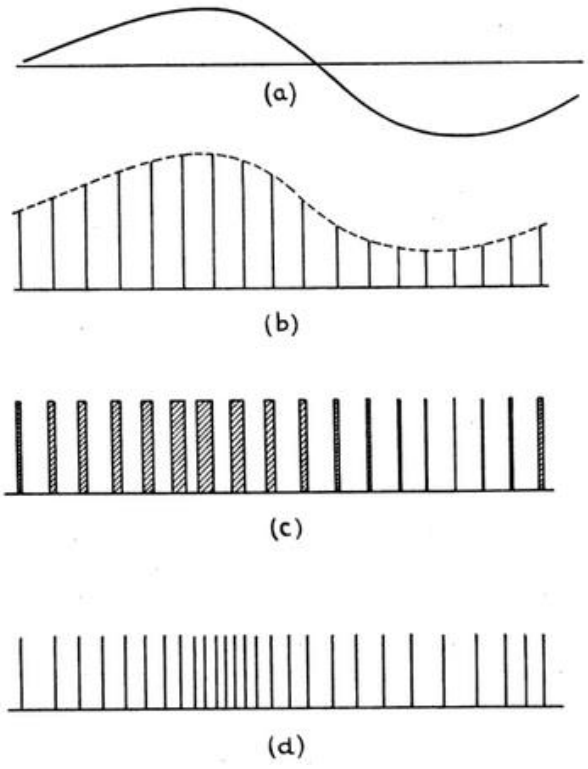

Figure 28 – Predicted output patterns (1950, Whitehead)

changes relative to the cycle of the modulating signal. Here, the spacing of the lines gets closer as the amplitude of the modulating signal gets higher, and further apart as it heads towards its negative peak. The spacing is more constant as the modulating signal is closer to zero. It can be noted that the lines in waveform (c) get thicker at the same time the lines in (d) get closer. The aim of testing this stage of the circuit is observe the changes to the amplitude and spacing of the quench waveforms under stimulation from an RF source and note similarities between the observed changes and the patterns demonstrated in Figure 28.

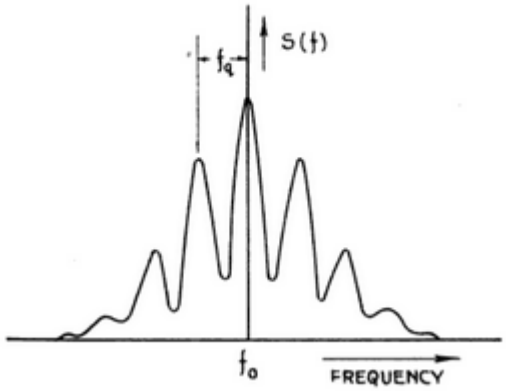

Figure 29 – Frequency response (1950, Whitehead)

Figure 29, taken from (1950, Whitehead) shows the frequency response of an SRR in its "coherent" state. The coherent state is a condition where all quench cycles are equally spaced, or coherently spaced. While this project does not make an intricately detailed study of an SRR's frequency response, the frequency response model detailed in Figure 29is a potentially useful model for analysing the RF radiation emitted by an SRR. It is stated in (2007, Insam) that as the self-oscillations build up, the SRR becomes a pulsed RF transmitter and considerable RF radiation escapes up the aerial in narrow bursts. This radiated frequency spectrum will be spread over a certain bandwidth at about twice the quench frequency.

Figure 29shows the quench frequency as f_q. The parameter S(t) represents the frequency spectrum along the y-axis and f_o represents the frequency along the x-axis. Frequency response can be simulated on LTSpice by using the Fast Fourier Transform (FFT) feature. Likewise, the frequency response of the actual RF radiation emitted by an SRR circuit can be analysed by using a spectrum analyser.

It is planned to test both the FFT on LTSpice and to analyse the final circuit using a spectrum analyser and look for similarities between their corresponding bode plots and the pattern in the bandwidth demonstrated in Figure 29.

4.1.4 Externally quenched SRR, predicted results.

The predicted results for the externally quenched SRR can be seen from the waveforms in Figure 9 and Figure 11. These demonstrate the effects of sinusoidal and square wave quench. As an externally quenched SRR produces these waveforms, the results are expected to follow these trends.

4.2 Simulation results

This section observes and analyses the results from the various simulations carried out during the design process. The simulations are conducted in 4 stages. First the oscillator will be simulated, followed by the super-regenerative oscillator. For the third stage an attempt is going to be made to simulate the effect of an RF signal on the circuit. Finally, a simulation of an externally quenched SRR will be made in an attempt to analyse the effect of different shaped waveforms from the external oscillator on the quench. All simulations are done using Linear Technology's LTSpice IV.

4.2.1 Simulation Results of Oscillator

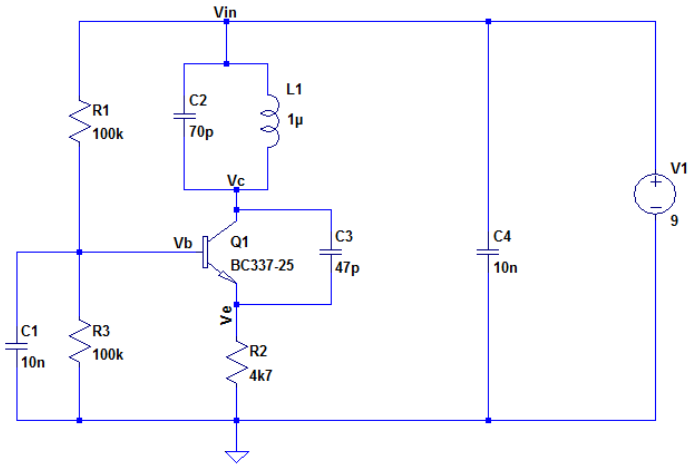

Figure 30 – Oscillator schematic.

2 main tests were carried out on the oscillator. Most important was the transient analysis. This type of test allows sinusoidal waveforms to be viewed on LTSpice's virtual oscilloscope. The main aim of the transient analysis test was to view the oscillations and observe how they changed as the value of C2, the main capacitor in the resonant tank circuit was altered. The second test to be undertaken was the DC operating point. This test displays all DC voltages in the system. The DC operating point is useful because it provides a guideline for measuring voltages in an actual circuit, which are useful when testing. All results for DC offset tests can be found in the appendix F. Figure 30 shows the schematic under simulation. The first test to be undertaken was a transient analysis of the voltages at the node Vc. Figure 31below shows the waveform

captured by this test. For the acquisition of this wave, C2 was set to 10pF. This test was repeated between a range of 1-80 pF in inclinations of 10pF.

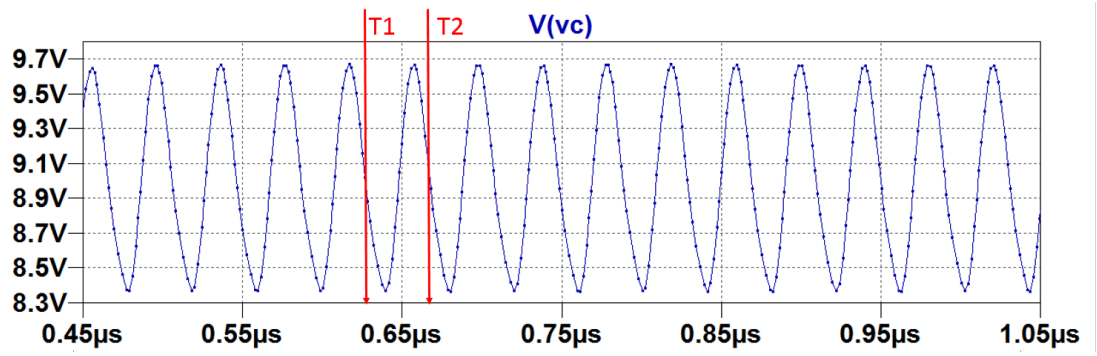

Figure 31 – Simulation result, oscillator.

The red arrows on Figure 31show the period of each wave cycle. T2-T1 is the amount of time it takes for the cycle to go through a full 360˚. From this time period, the frequency of the wave can be calculated using the formula T=T2-T1 and f=1/T where T is time in µs an f is frequency in Hertz. The table below, figure shows the measured frequency and the value of capacitor C2, with C3 at values 4.7 pF and 47pF.

The chart on the next page, Figure 32 plots the capacitance against the frequency the oscillator produces. While it follows the same pattern as the chart in Figure 15, with the frequency rising as the capacitance falls, its results are not consistent with the predicted results. First of all, the frequencies produced are far lower than those predicted. Secondly, the gradient at which the curve drops is far less steep on the recorded results than on the predicted. As the capacitance goes up, the results correlate less and less. While higher capacitances such as 60-80 pF are maybe 10 MHz different to the predicted result, the frequency of the oscillator at lower capacitances is sometimes as much as six times lower than predicted. Another factor was that after the capacitance hit a certain level, the circuit ceased to oscillate.

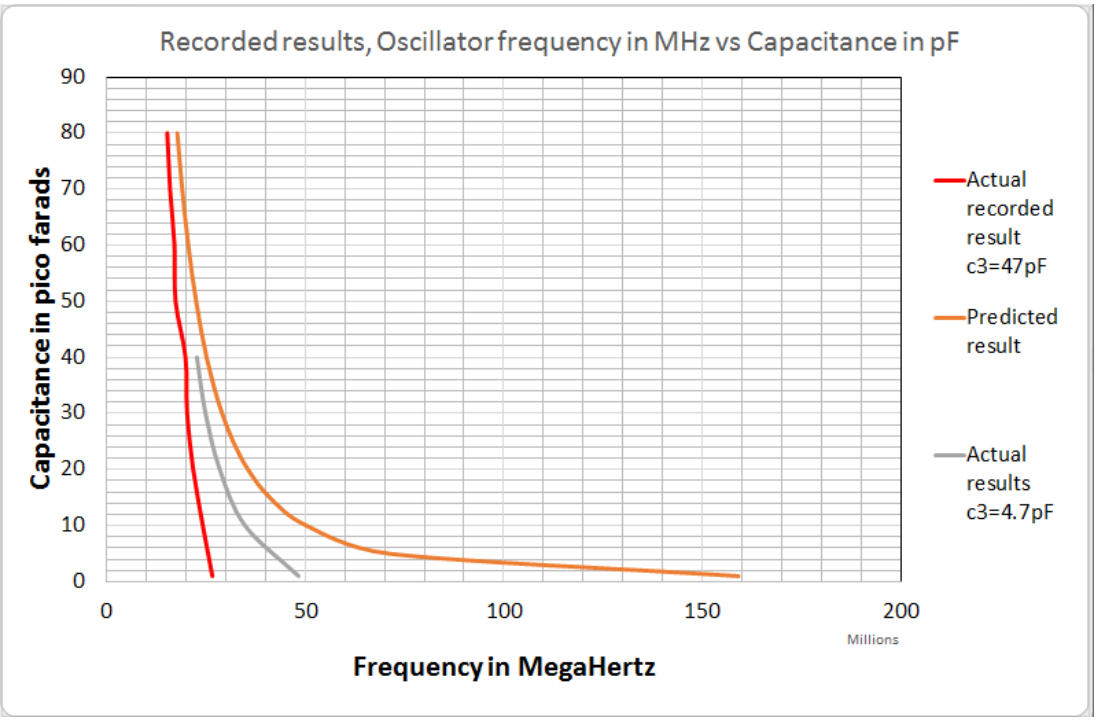

Figure 32 – Predicted and actual results from oscillator.

As a result of this, the test was repeated with C3 having a value 10 times lower (4.7pF). The results of this test were more consistent with the predicted results, however, the oscillations ceased when the capacitance of C3 was raised above 40pF. This test was repeated because on the original ugly build oscillator, the value of c3 was 4.7 pF, whereas on the final circuit it was 47pF. The table of results from the DC operating point simulation can be f.

4.2.2 Simulation Results of super-regenerative oscillator

As with the previous section, transient analysis and DC operating point simulations were carried out. The transient analysis was repeated at the value of resistor R2 was increased in 1kΩ increments. The effect on the frequency of the quench oscillations was then observed. Observations were also made on the effect of the frequency in the tuned oscillator. The value of C4 was adjusted and any changes to the waveform were

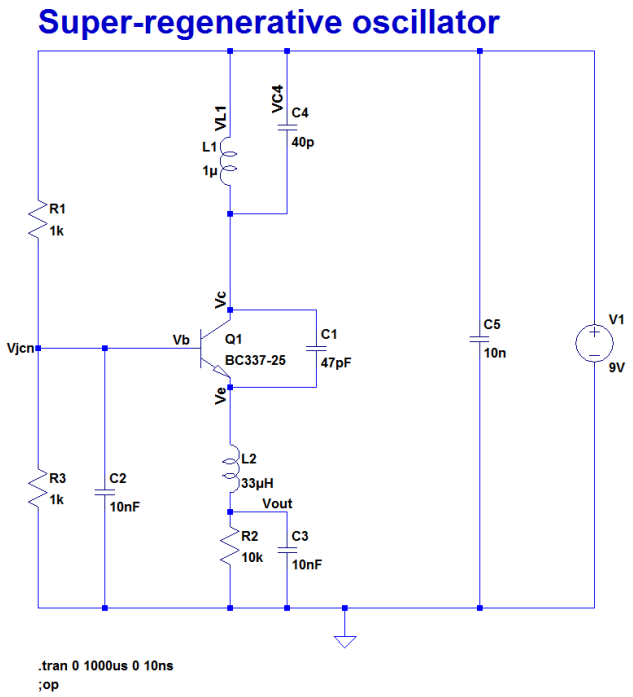

Figure 33 – Super regenerative oscillator.

noted. Finally, a simulation was carried out using LTSpice's Fast Fourier Transform simulation (FFT).

In the first test, to observe quench, voltage measurements were taken from the nodes Vc at the collector of the transistor, Vb at the base of the transistor, Ve at the emitter of the transistor and Vout. All of these points are marked on the schematic in Figure 33. Another transient analysis was then run to measure the currents in the transistor as well as R1, R3, C2 and R2.The waveforms in Figure 34show the results of the first

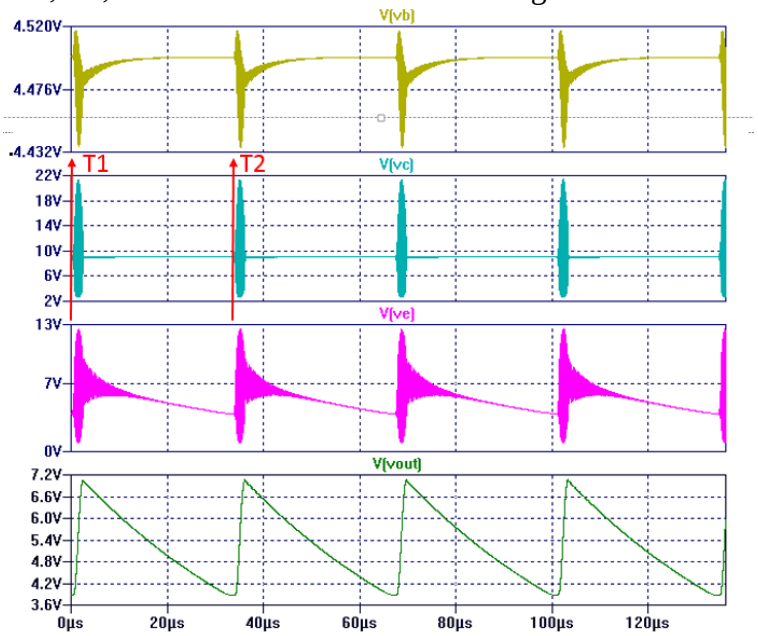

Figure 34 – Quench waveforms

transient analysis test. The circuit had C4 set at 5pF and R2 set to 5kΩ when this test was conducted. The test was repeated with R2 set between 1-10kΩ in 1kΩ increments. The test was then repeated again with C4 set to 50pF. The red lines labelled T1 and T2 show the 2 points which make the period of one quench cycle. This can be used to calculate the quench frequency. The table below, shows the change in quench frequency, the value of R2 and the Vpk achieved by the quench waveform at Vc.

R2 value in kΩ	Quench frequency f_q in Hz with C4 at 5pF	Quench frequency fq in Hz with c4 at 50pF	Vpk at Vc C4=5pF	Vpk at Vc C4=50pF
1	121654	Quench collapse	22.2	17.6
2	66844	67294	22	17.31
3	46772	48449	21.65	17
4	36549	38865	21.65	17
5	29524	32082	21.47	17
6	25113	27314	21.47	17
7	21706	23854	21.3	17
8	19146	21199	21.3	17
9	17164	19018	21	17
10	15271	17196	20.94	17

Table 1 – Quench Frequencies

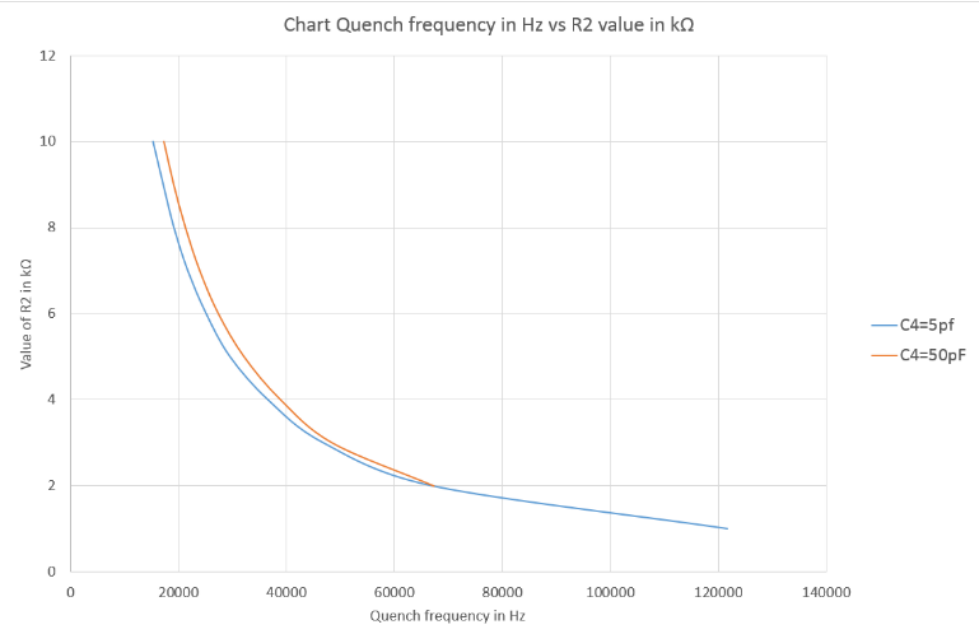

Figure 35 – Quench frequency chart

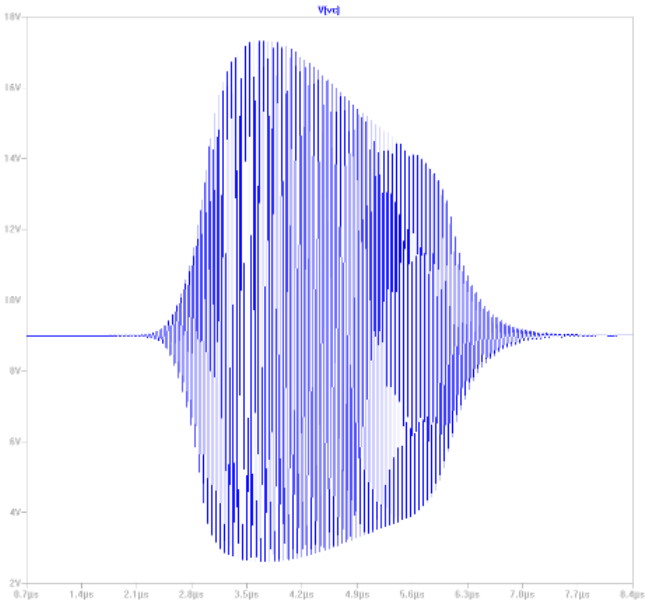

Figure 36 – Zoom in on quench waveform

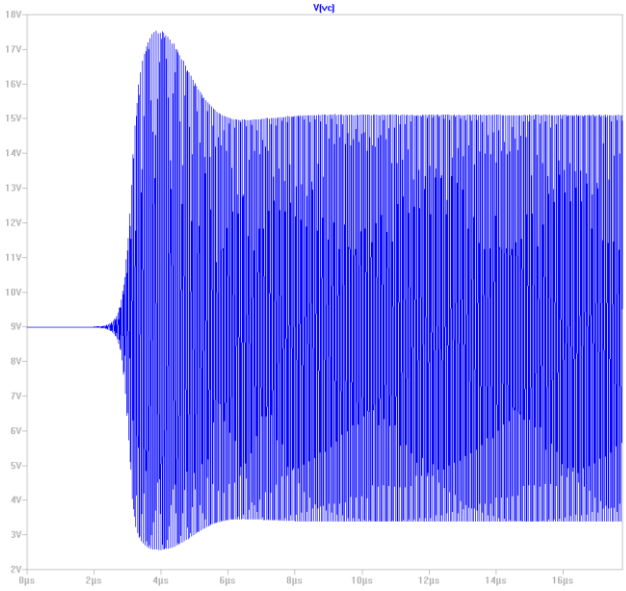

Figure 37 – Quench collapse

The chart above, Figure 35, shows the non-linear trend of quench frequency increasing as the value of R2 decreases. When C4 was set at 50pF, the quench collapsed when R2 was set to 1kΩ, but, until that point, the difference made by changing the value of C4 was minimal. The waveform in, Figure 37, demonstrates what happens when the quench collapses. This measurement was taken from Vc. The oscillation will build up, however, it is unable to decay again. At this point, the peak voltage was also slightly higher than at previous values of C4.

The waveform in Figure 36is a close up of a quench oscillation. A quench is essentially a series of oscillations within an oscillation. Oscillations build up and decay at a certain frequency (the quench frequency), meanwhile they oscillate at the frequency created by the tuned oscillator.

The waveforms in Figure 38show the current measurements from the circuit Figure 33. On the bottom pane, Vc has been included to add a reference point, to observe where these fluctuations in current happen relative to the quench. The most notable observation here is how the base voltage follows the current through R3.

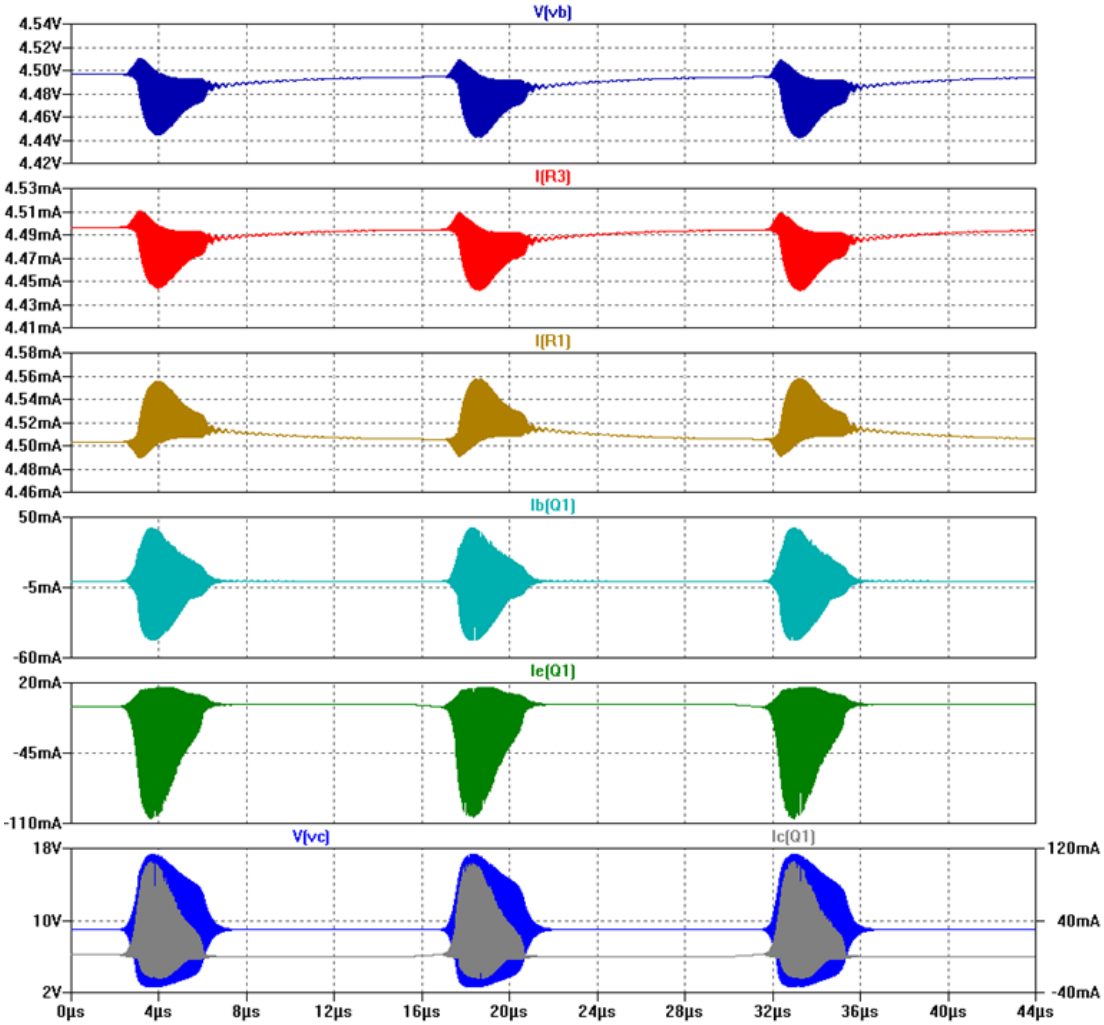

Figure 38 – Current measurements from SRO

The table in appendix F shows the DC operating point for the circuit shown in Figure 33. The waveforms on the next page (Figure 39, Figure 40, Figure 41, Figure 42) show the frequency response of the circuit shown in Figure 33, acquired using the Fast Fourier Transform (FFT) in LTSpice. Figure 39 shows the FFT with a linear x axis, while Figure 40 shows the same readings with a logarithmic x-axis.

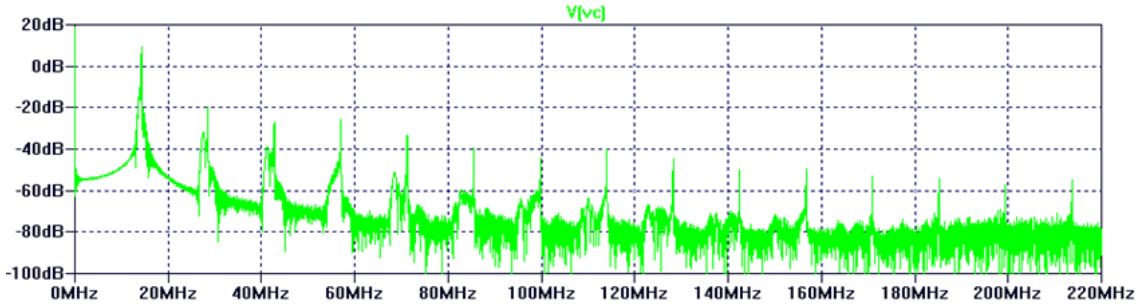

Figure 39 – Linear frequency response dB

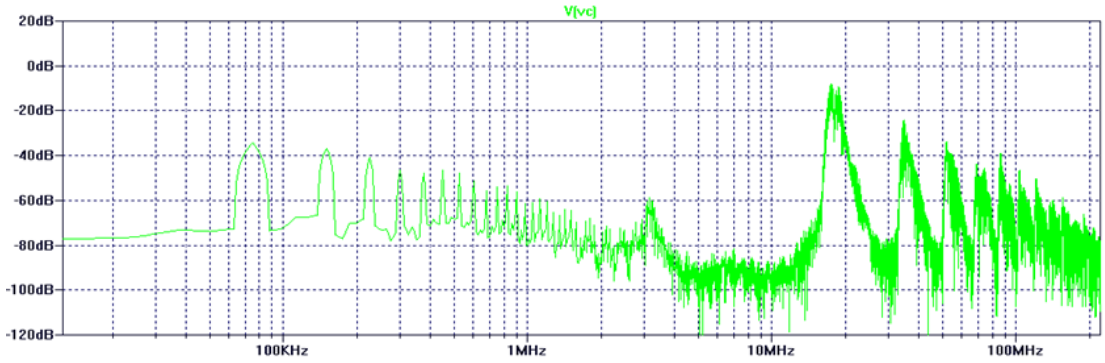

Figure 40 – Logarithmic frequency response dB

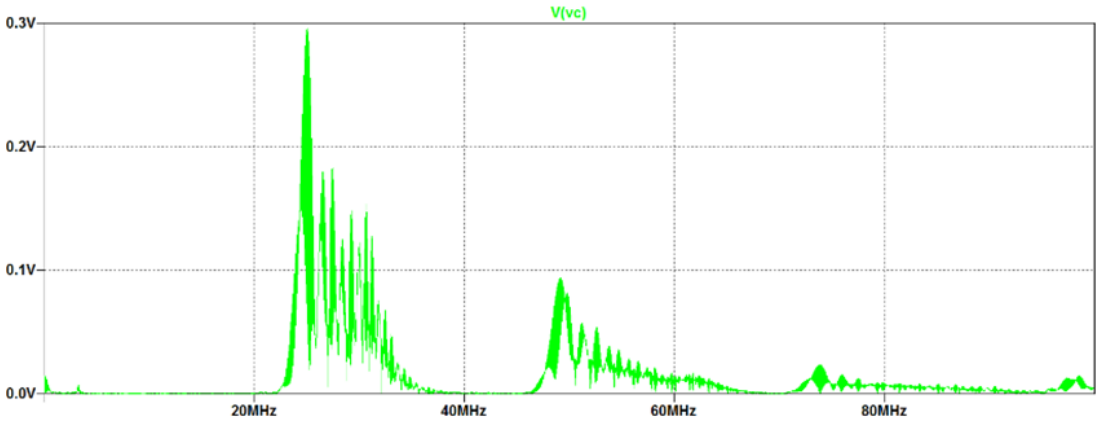

Figure 41 – Linear frequency response, Volts

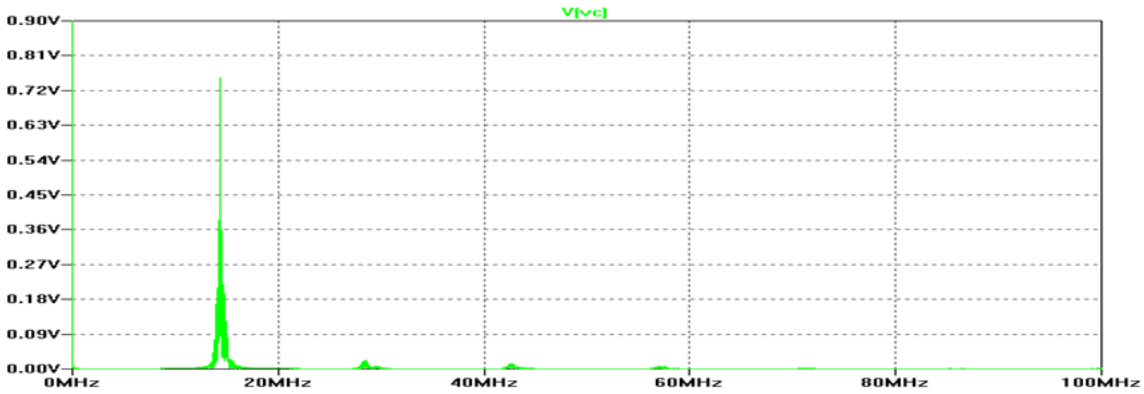

Figure 42 – Linear frequency response, Volts, low frequency

For the tests in Figure 40 and Figure 41, R2 was set to 2k for high frequency quench and C4 was set to 5 pf. Further analysis showed little change to the waveforms when quench and C4 were changed, however, when a purely linear test was carried out, once with C4 set at 1pF and once at 100pF there was a noticeable change.

Figure 41 shows the results with C4 at 1pF and Figure 42 shows the results with C4 at 100pF. While the magnitude of the peak at 100pF was much higher, at 1pF, the sidebands were more prolific. They were also much further spread, ranging from approximately 21 MHz to almost 100 MHz, as opposed to about 15-56 MHz when C4 was set to 100pF.

4.2.3 Simulation of super regenerative receiver with RF stimulus.

In this section, an attempt was made to simulate an incoming RF signal and observe its effect on the quench. Figure 44shows the transient analysis results of a test applying a simulated FM signal to the system. These were acquired from the simulation shown in Figure 43. The signal had a modulating frequency of 10 kHz and a carrier frequency of 20.6MHz. Interestingly, Ve has adopted the waveform from the FM from an SFFM voltage input, while Vc adopts an AM like wave form. Vout ceases its saw tooth waveform and adopts characteristics of both the FM wave and the quench.

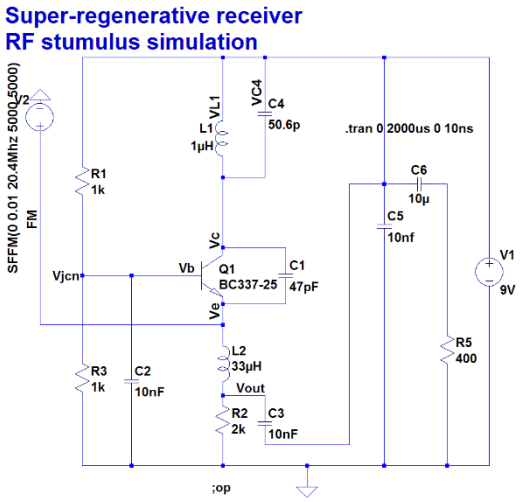

Figure 43 – FM simulation

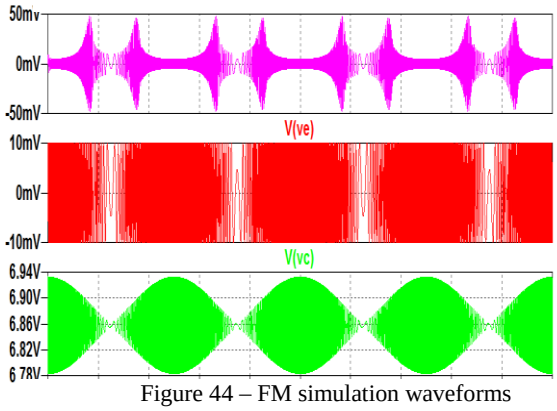

Figure 44 – FM simulation waveforms

Figure 45 shows the waveforms acquired from the AM signal test. In this test the quench from Vc and the waveforms from Ve and Vout remain unchanged, however, the incoming AM waveform seems to

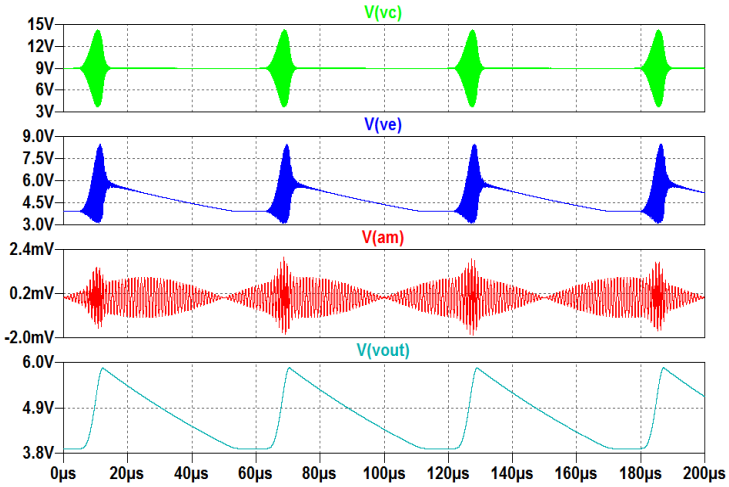

Figure 45 – AM simulation waveforms

have voltage spikes which correlate with the position of the quench waveforms. This was an unexpected result, however, it explains the purpose of quench well- only the parts of the AM waveform affected by the quench will be received, hence, the sampler like quality of a quench waveform. Increasing the frequency of the quench would increase the amount of signal sampled and as a result, increase its fidelity.

4.2.4 Externally quenched SRR simulation results

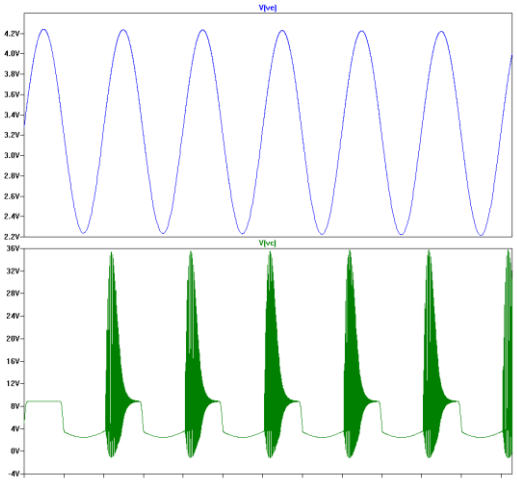

Figure 46 – Externally quenched, voltage controlled waveforms

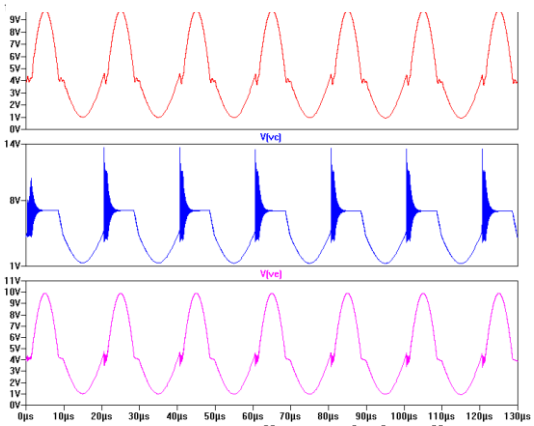

Figure 47 – Externally quenched oscillator waveforms, current controlled

This section looks at the results from the externally quenched SRR deigns explained in section 3.4. Most simulations of the externally quenched SRR proved inconclusive, however, the test using a current and voltage source shown in Figure 23 produced some waveforms that were slightly consistent with the predicted outcome. Figure 46 shows the wave forms acquired from a transient analysis on this circuit. The sine wave shown at the top is the emitter voltage. This is the same waveform applied from the voltage source which acts as the external oscillator. The waveforms at the bottom are from the collector. They show the distinct pattern of quench, however, unlike the self-quenching version, once the oscillations have stopped, the voltage does not return

to a constant level. Figure 47 shows results from the test done using a current source as an external quench oscillator. The voltage from the emitter shows the quench waveform, but with a faster gain than the voltage controlled version. Likewise, the emitter voltage has a small oscillation when each cycle goes through 0˚.

4.3 Final Circuit Test Results

This section details the test procedures and final results for all hardware built for this project. One of the key measurements taken in all tests was the effect of the change in capacitance. The variable capacitors used were TTWM 2 gang variable capacitors. The TTWM is controlled by a dial which can rotate through 180˚. The table below shows the percentage of rotation against the capacitance for the units 2 settings, A-G and O-G.

Rotation %		100	90	80	70	60	50	40	30	20	10	0
Capacitance in Pico farads	Set 0-G	59.2	55.2	50.9	46.2	41	35	28.4	21	12.9	4.8	0.3
	Set A-G	141.6	126.3	111.2	96.1	80.4	64.3	48.5	33.2	18.5	6.2	0.3

Table 2 – Variable capacitor settings

The following table lists equipment used

Tektronix DPO 3054 4-channel Digital Oscilloscope	Hewlett Packard 8560-E Spectrum analyser
Rapid HY 3002-3 DC Power supply	Samsung S6810P Galaxy Mobile phone with FM radio app.
Fluke 6061 E RF generator	GW Instek SFG-2104 Signal Generator

Table 3 – Equipment used

4.3.1 Oscillator test, experimental procedure

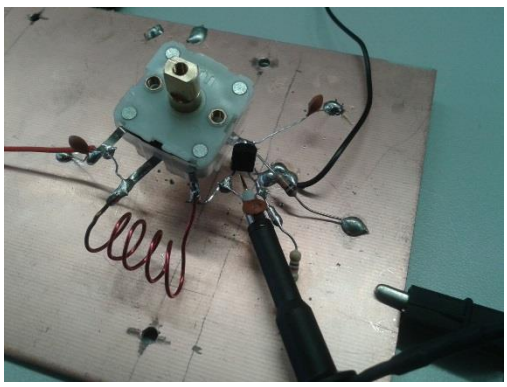

Figure 48 – Oscillator testing

The first stage of this test was to test the ‘ugly build’ oscillator. The unit was powered by a Rapid HY 3002-3 Dc bench power supply and tested using a Techtronix DOP 3000 digital oscilloscope. The image in Figure 48 shows the oscilloscope probe attached to the collector of the transistor. In this experiment, it was important to attach the probes to the insulated part of the wire instead of the live

part. This is because the probe was detecting the RF oscillations from the oscillator and not the voltages in the system. Attaching the probe to a live wire would cause the oscillation voltage to collapse, giving only a DC operating point reading. The capacitor was then adjusted and the change in frequency was noted. The oscillator was tested with the capacitor set at both A-G and A-O. This was done by disconnecting it from one terminal then re soldering it to the other. The varicap was then adjusted in revolutions of 45˚. The approximate capacitance was then estimated from the readings in table 2.

4.3.2 Oscillator test results

The image in Figure 49 shows the waveform measured from the oscillator using the oscilloscope. It shows a sine wave with a frequency of 62.5Mhzand a Vpk of 200mV.

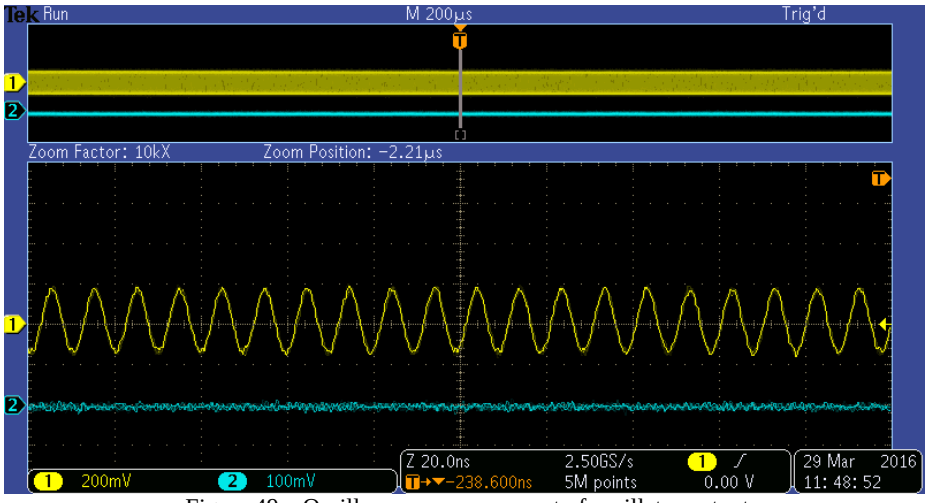

Figure 49 – Oscilloscope measurement of oscillator output

The table below shows the recorded frequencies against the estimated capacitance.

A-G	0.3	58	
A-G	64.3	45.5	
A-G	80	40	Oscillations begin to deteriorate
A-G	105	26.3	Last measurable parameter before oscillations collapse
A-G	141.6	0	
O-G	0.3	90.9	
O-G	21	80	
O-G	35	62.5	Waveform photographed in figure 54
O-G	48	52.6	Oscillations deteriorate
O-G	59.6	50	

Table 4 –Oscillator results

The results in Table 4 show some inconsistencies. Theoretically, for the setting on the varicap when the capacitance was at it's lowest, the frequencies for A-G and o-G should have been similar.There are 2 possible reasons for this inconsictency. First of all, the lowest value of capacitance stated in the manufacturers literature may have inconsistencies. Secondly, the value of the inductor can be altered by stretching and compressing it. This is a possibility due to the fragile nature of the ugly build oscillator.

The notes in table 4 mention the deterioration and eventual collapse of oscillations. This was more of an issue with the varicap set from A-G. At the lower frequencies, the waveforms would become distorted and eventually stop oscillating. While the waveforms would lose their perfectly sinusoidal shape at lower frequencies with the varicap set from O-G, they never stopped oscillating completely. The image in Figure 50shows a waveform at a lower frequency showing signs of distortion. This waveform is at 35.7Mhz, the point where the distortion started.

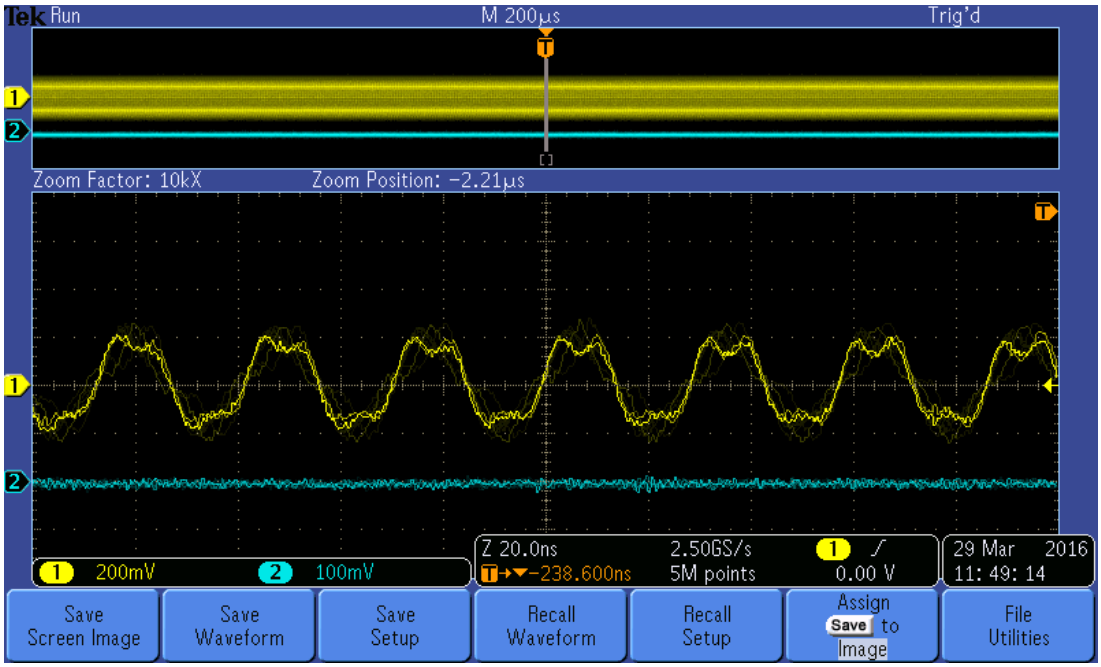

Figure 50 – Distorted oscillation

This experiment was repeated on the circuit described in figure 23. No real measurements were taken during this test, as it was mainly carried out as part of the testing during construction procedure, however, as there were substantial differences in some of the component values of the ugly build oscillator and the tuned oscillator in the final circuit, the waveforms were much more distorted and unstable. The image in Figure 51show a waveform taken from one of these tests.

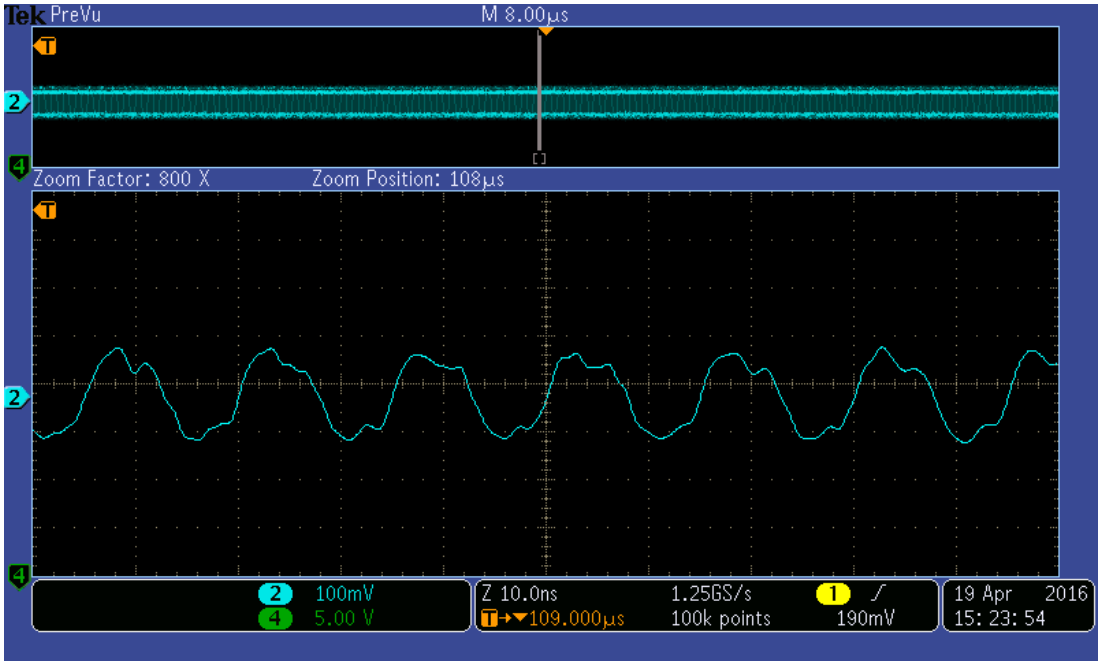

Figure 51 – Distorted oscilation

4.3.3 Super-regenerative receiver, experimental procedure

This section covers the testing of both the super-regenerative oscillator and the final receiver. This stage of the testing was broken down into 5 separate tests.

1. Test SRO with oscilloscope and look for quench waveforms.
2. Attach aerial and audio output and detect a signal.
3. Use the RF signal generator to generate a 400/1000Hz modulating signal with a variety of carrier signals and observe effects on oscilloscope/ listen for detection of audio signal.
4. Tune a radio to a certain frequency then tune SRR to the same frequency and observe the distortion caused by RF radiation.
5. Test RF radiation using a spectrum analyser.

The oscilloscope used for this experiment was a Tektronix DPO-3054. This piece of equipment was necessary because it can operate at up to 500MHz, as opposed to the 40MHz limit of a standard CRO. As the oscillator was designed to operate at 100+MHz, a standard CRO would not have been adequate for work at this kind of frequency.

As with the tests in the previous section, the oscilloscope was looking for RF frequencies, not voltages in the circuit itself. As a result, all probes had to be attached to either the insulation on the wire or placed near the node they were taking the measurement from, but not actually touching it. Figure 52 shows the experimental set up for this test. The yellow text boxes show the parameters each probe is measuring.

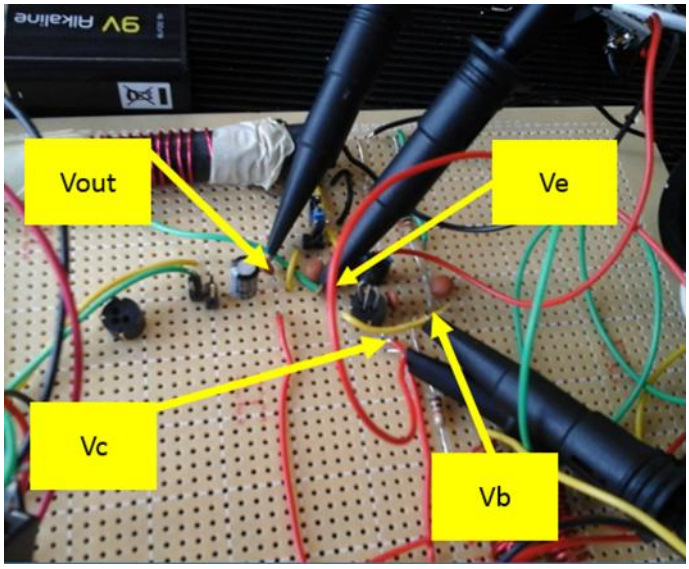

Figure 52 – Test setup

4.3.4 Super-regenerative receiver test results

The first test done with the SRR was to observe quench waveforms using the oscilloscope. The image in figure 58 shows the waveforms captured in this initial test.

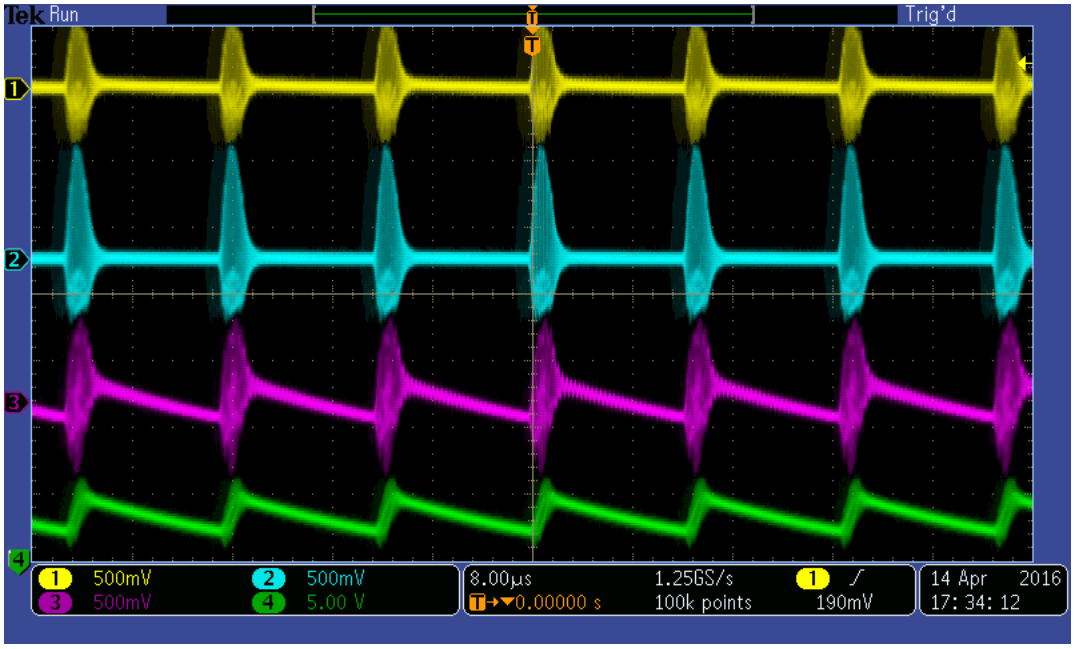

Figure 53 – SRR oscilloscope readings

The yellow waveform at the top shows the measurement from the base of the transistor (Vb) and the Blue wave below it is a measurement from the collector (Vc). These waveforms both demonstrate quench. The purple waveform is from the emitter, while the green waveform at the bottom is from Vout (see figure 23 for node locations). As with the simulation tests, altering the resistance at the emitter, in this case altering VR1, and VC1 changed the frequency of the quench. In the case of the waveforms in figure 58, the quench frequency is about 83MHz.

The next test involved attaching the aerial and the audio output. This test was done twice, once through output 1 straight into the 1W stereo amplifier and the second time through the output 2, which included the pre amp and low pass filter stage. The radio detected a signal in both instances. The audio quality from output 1 was very quiet, however, the output though the pre amp and o/p 2 was much louder and clearer. While this test proved it worked, it didn't say much about what was actually happening inside the radio. While an oscilloscope could detect the differences in the quench, no real data could be acquired from this test.

The next stage was to detect RF signals from a controlled source. For this, a Fluke 6061A RF signal function generator was used. This device can produce both AM and FM radio frequencies at up to 1GHz. The FM radio on a mobile phone was used to calibrate this test by tuning into the frequencies generated by the SFG. An oscilloscope was used to measure the results of this experiment. Channel 4 from the oscilloscope was attached to the output of the SFG for testing AM, while Channel 1 was attached to the audio output and channel 2 was attached to Vc.

The signal function generator was set to 15dBm with an AM carrier frequency of 101.1MHz. The varicap on the tuner was set to approximately 64pf. The quench was set quite high, with the value orVR1 being about 2kΩ. Figure 59 shows the recorded waveforms, with a modulating signal of 400Hz. The unexpected result here is that while the output and input show characteristics of FM, the quench shows characteristics of FM, with the frequency modulation decreasing as the amplitude of the AM wave gets higher. During this test the 400Hz audio signal carried by the modulating signal was clearly audible. The next test was to analyse the effect of FM waves on the receiver. An FM wave of 100MHz was generated. Figure 60 shows the effect an FM wave has on the quench waves.

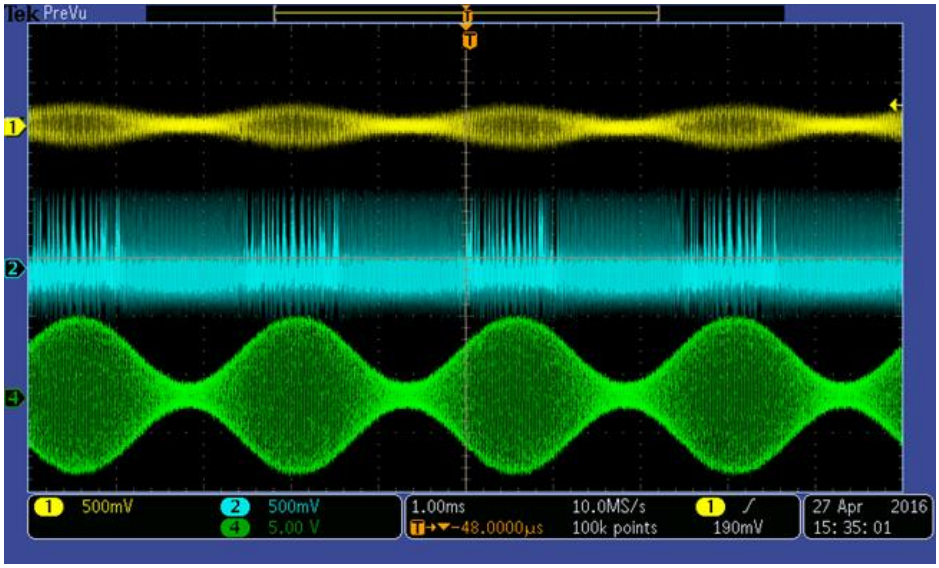

Figure 54 – Oscilloscope waveform, AM signal

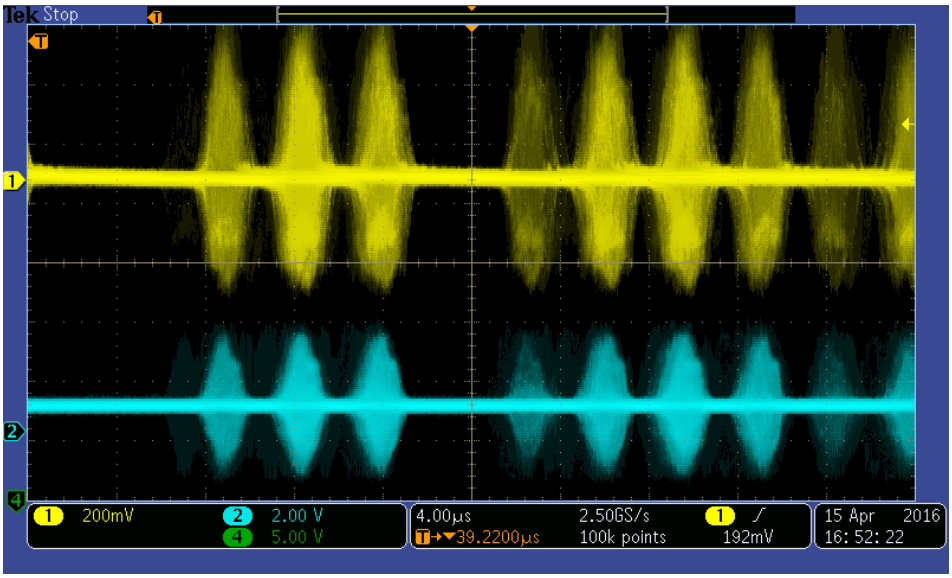

Figure 55 – Oscilloscope reading, FM stimulus.

The blue lines show the waveform from the audio output, while the yellow waveform is from Vc. No input signal was recorded in this test because the waveforms were of such a high frequency that they were unreadable on the oscilloscope setting needed to measure quench. With the FM test, the audio signal contained in the modulating signal was very hard to detect. First of all, there was a lot more static in the FM detection than in the AM detection. Secondly, whenever the audio signal was detected, it was only for very brief intervals.

To test the RF generator was working correctly, the SRR was switched off and 105.6 FM was tuned into using a mobile phone radio. The RF generator was then set to the

same frequency. The RF generator drowned out the station the phone radio was tuned to and the audio signal became audible. The Phone radio could detect the signal from the RF generator up to about 20 or so meters away. Next, the SRR was tuned to what was estimated to be 105.6 FM. This caused considerable interference with the phone radio up to a range of about 5 meters away.

This was substantial proof as to the SRR's ability to cause interference through RF radiation. The next stage was to obtain physical evidence of this radiation. This was done using a spectrum analyser. The images in figures Figure 56, Figure 57, Figure 58,Figure 59 show the readings from the spectrum analyser with the measurement probe placed next to the SRR. In Figure 56 the SRR is switched off, meanwhile in Figure 57 the SRR is switched on and the two sidebands are noticeable, while in Figure 56 they are absent.

Figure 63 and 64 show the same readings, but with the reference line set to -5.6dBm. In both of these images, the quench is set as high as possible without collapsing. In Figure 63, the SRR was set to the point where it would interfere with an FM radio tuned to 105.6MHz FM. In Figure 64 it was tuned to the point where it would interfere with an FM radio tuned to 88MHz. There is a noticeable difference in the amplitude and number of sidebars. This could possibly explain a phenomenon observed during the audio testing. When quench is set to certain levels, the audio frequency broadcast from the RF could be heard at different levels over quite a large amount of tuned bandwidth.

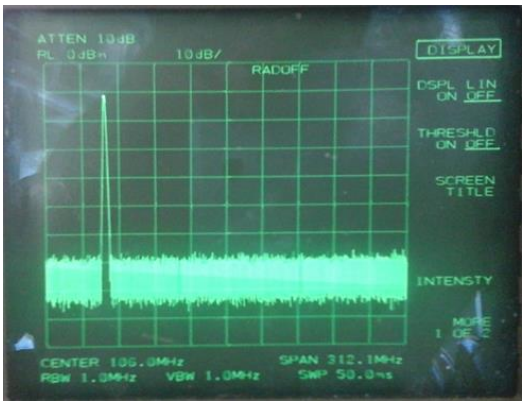

Figure 56 – Spectrum, SRR off.

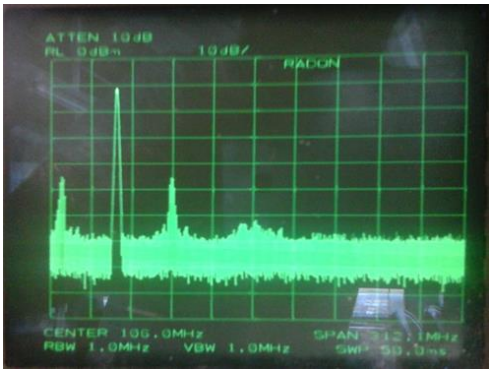

Figure 57 – Spectrum SRR on

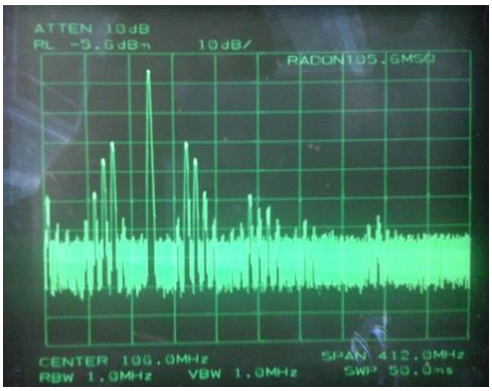

Figure 58 – Spectrum, 105.6MHz SRR ON

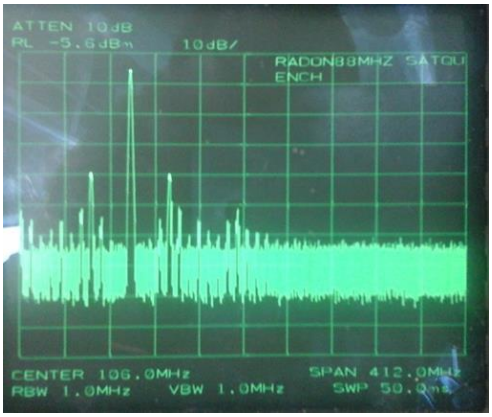

Figure 59 – Spectrum 88MHz SRR ON

When the quench was ajusted to a higher frequency, the tuning became more precise, and the audio signal could only be heard at a very specific tuning. More interestingly, at certain quench settings, a signal could be detected well at several settings, and not at all at several others.For instance, if the dial on C4 was rotated to 20°, then to 45° degrees then again to 60°, the signal could be detected, but not at any other settings inbetween. A similar effect was observed when distorting the FM radio. There was a range of settings which could distort another radio tuned to a specific frequency.

Chapter 5.0 Conclusion

5.1 Critical Reflection

The test results on the super-regenerative radio have produced some surprising results. While a lot of the theory, simulation and test results have been conclusive with each other, some other results have been in-consistent with the predictions.

The oscillator results followed the predicted pattern expected, in that, as the capacitance was decreased, the frequency increased. The major inconsistency with both the simulation and the test is that the frequencies achieved were not as high as those predicted. There could be several reasons for this. The most likely reason is that while the equation:

$$f = \frac{1}{2\pi\sqrt{LC}}$$

Is based around ideal conditions, the practical circuit is not. The equation above only considers the inductor and capacitor as components which affect the outcome of this circuit, however, there are several resistors and resistive, inductive and capacitive elements of the transistor which are not considered by this equation. These could ultimately have an effect on the overall frequency as additional capacitance and inductance which is not accounted for ultimately affects the outcome of the equation.

The results with the super regenerative oscillator were much more consistent with the predicted results. Both simulation and tested circuit produced similar waveforms. Likewise, changing the value of the variable resistor coming from the emitter changed the frequency of the quench in both the simulation and the circuit tests. The chart in **Error! Reference source not found.** demonstrates the correlation between the recorded quench frequencies from the simulation in section 4.2. The recorded frequencies are slightly lower than the simulated frequencies, but follow the same trend of increased quench frequency with decreased resistance.

Its correlation with the simulation where C4 was set to 50pF was much closer, with details such as the quench collapsing on the simulation after exceeding 67 kHz on the simulation and 50 kHz in the test.

In the circuit tests, quench has a very important effect on reception of a signal. Even the slightest change in quench frequency can dictate whether a signal is received or not.

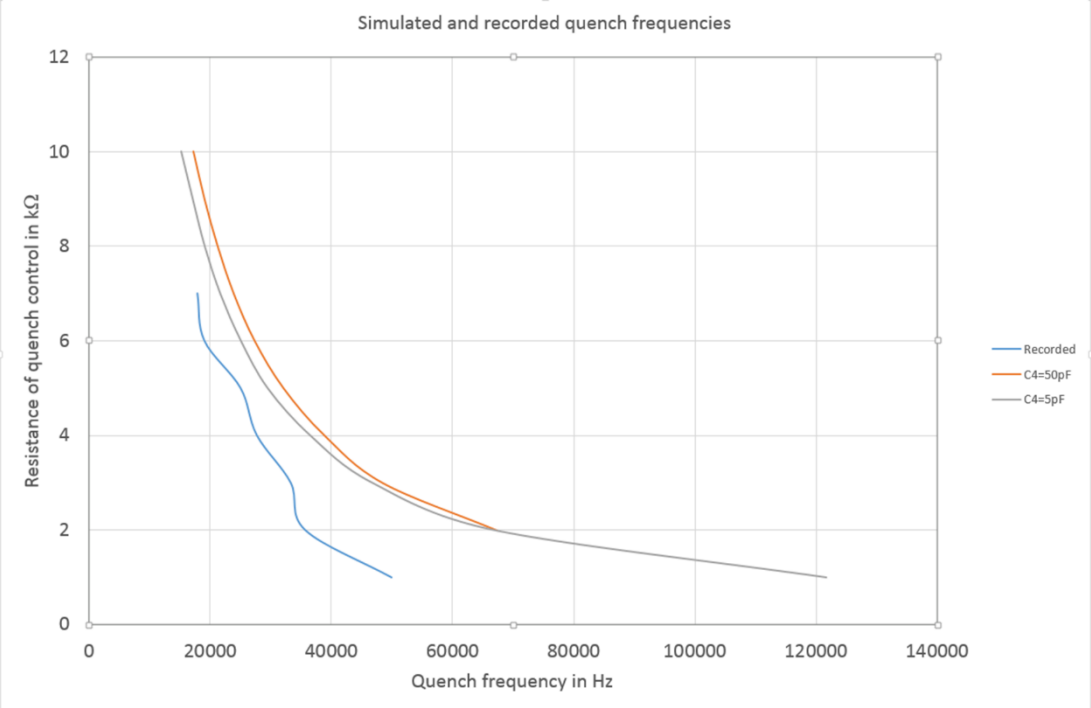

Figure 60-Quench frequencies

While the principle behind simulating quench seems straight forward, the principle of simulating its effect on the reception of an RF signal is not. The results from the circuit tests and the simulations seemed to contradict each other.

While the simulation seemed to suggest that an FM signal would give rise to an AM like wave form in the quench oscillations, the actual response from the quench in the circuit test bore more resemblance to the predicted results from (1950, Whitehead),shown in **Error! Reference source not found.**. The waveforms shown below in **Error! Reference source not found.** show the spacing between quench

oscillations changing under stimulus. Note the uneven spacing in the quench oscillations, as mentioned in figure 5.

The simulation results also seemed to suggest that an AM frequency would have no effect on the quench.

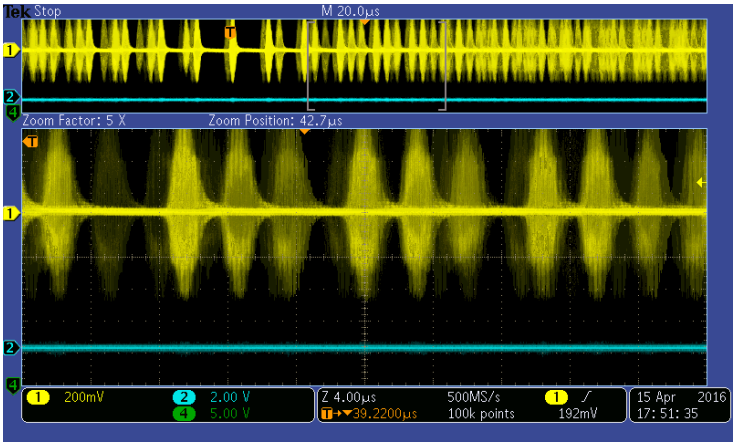

Figure 61-Quench under FM stimulus.

The circuit test results with AM RF stimulus seemed to disprove this, with some tests suggesting that an AM stimulus would give rise to an FM like quench waveform, such as the waveforms demonstrated in Figure 54.

The tests using the spectrum analyser not only gave clear evidence that the SRR gives of considerable RF radiation, but the change in the spectrum when the tuning was adjusted also raised an interesting area of enquiry. In section 4.3 it was mentioned that audio during testing some frequencies could be detected on more than one tuner setting. Looking for a correlation between these two phenomenon could prove to be an interesting line of future enquiry.

While some aspects of this project could be considered to be relatively successful, there are several improvements which could have been made. First of all, the relative inaccuracy of a lot of measurements made has only allowed the acquisition of data that gives a general over view of the operation of an SRR, rather than a detailed analysis. Secondly, the design could have been more refined and advanced upon, as the working circuit still has several major drawbacks such as relative inaccuracy of tuning and poor sound quality. Another issue is a possible mal-function in the pre amp section which could be addressed.

The attempts at simulating RF signals in the system could have been more effective, a possible improvement on these experiments would have been to use a non-periodic waveform and observe the effect it has on the quench. This is because in a real world radio signal, repetitive sinusoidal signals would be a rare occurrence.

5.2 Further study

Despite the shortcomings of this project, it has given a good insight into the workings of RF systems and indeed, RF theory as a whole. Apart from trying to improve and further the design, another interesting line of study would be to look into alternative uses for SRRs.

Radio is an integral part of modern technology. Modern systems such as Bluetooth and Wi-Fi depend on it, as do an emerging number of remotely controlled vehicles. The low component count of an SRR makes it an ideal circuit to be miniaturised. Miniaturisation of circuits is a key factor in hand held devices such as phones, tablets and small remote controlled vehicles. Researching the applications an SRR could possibly have in these rapidly evolving fields would be the most logical next step onwards from this research.

References

F, C. W. 1958. *Super regenerative detector using transistors*.

Insam, D. E. 2002. *Designing super-regenerative receivers* [Online]. Available: http://www.eix.co.uk/Articles/Radio/Welcome.htm [Accessed].

Kainka, B. 2007. *FM Super-regenerative receiver* [Online]. Available: http://siva666siva.webs.com/fm.pdf [Accessed].

Otung, I. 2001. *Communication engineering principles,* Basingstoke, Palgrave.

Whitehead, J. R. 1950. *Super-Regenerative Receivers. [With plates.],* Cambridge, Cambridge University Press.

Workshop, D. Z. *TTWM_variable_capacitor* [Online]. Available: http://www.mzentertainment.com/technical_archive/TTWM_variable_capacitor.gif [Accessed 5 May 2016].

www.circuitsgallery.com. *Matlab code for AM* [Online]. Available: http://www.circuitsgallery.com/2012/05/matlab-code-for-amplitude-modulation-am.html [Accessed 5 May 2016].

www.circuitsgallery.com. *MATLAB code for FM* [Online]. Available: http://www.circuitsgallery.com/2012/07/matlab-code-for-frequency-modulation-fm.html [Accessed 5 May 2016].

(Insam, 2002, www.circuitsgallery.com, www.circuitsgallery.com, Otung, 2001) (Kainka, 2007, F, 1958, Insam, 2002, Whitehead, 1950, Workshop)

Bibliography

F, C. W. 1958. *Super regenerative detector using transistors*.

Fernandez, F. 2008. Super regenerative receiver. Available: ece.tamu.edu/~sanchez/665%20SRR%20Fall08.pdf.
Frey, D. R. 2013. Improved Super-Regenerative Receiver Theory. *IEEE Transactions on Circuits and Systems I: Regular Papers,* 60**,** 3267-3278.
Insam, D. E. 2002. *Designing super-regenerative receivers* [Online]. Available: http://www.eix.co.uk/Articles/Radio/Welcome.htm [Accessed].
Kainka, B. 2007. *FM Super-regenerative receiver* [Online]. Available: http://siva666siva.webs.com/fm.pdf [Accessed].
King, G. J. 1977. *Radio circuits explained,* London [etc.], Newnes Technical Books.
Lathi, B. P. 1983. *Modern digital and analogue communication systems,* Tokyo, Holt-Saunders Japan.
Ludwig, R. & Bretchko, P. 2000. *RF circuit design : theory and applications,* Upper Saddle River, NJ, Pearson Education.
McFarlane, G. G. 1947. *The Theory Of The Super-Regenerative Receiver Opererated In The Linear Mode* [Online]. Available: http://ieeexplore.ieee.org/stamp/stamp.jsp?arnumber=5298986 [Accessed 22/04 2016].
McGregor, I. & University of, G. 2008. *Low power RF transceivers,* Glasgow, University of Glasgow.
Otung, I. 2001. *Communication engineering principles,* Basingstoke, Palgrave.
Petruzzellis, T. 2008. *22 radio receiver projects for the evil genius,* New York ; London, McGraw-Hill.
Rohde, U. 2001. *Communications Receivers*, McGraw Hill.
Rojas, R. F. a. O. 1997. Modelling and simulating the super regenerative receiver. Available: http://server3.eca.ir/isi/forum/Modeling_and_simulation_of_the_superregenerative_receiver.pdf.
Schetgen, R. & American Radio Relay, L. 1992. *The ARRL handbook for radio amateurs,* Newington, CT, American Radio Relay League.
Whitehead, J. R. 1950. *Super-Regenerative Receivers. [With plates.],* Cambridge, Cambridge University Press.
Workshop, D. Z. *TTWM_variable_capacitor* [Online]. Available: http://www.mzentertainment.com/technical_archive/TTWM_variable_capacitor.gif [Accessed 5 May 2016].
www.circuitsgallery.com. *Matlab code for AM* [Online]. Available: http://www.circuitsgallery.com/2012/05/matlab-code-for-amplitude-modulation-am.html [Accessed 5 May 2016].
www.circuitsgallery.com. *MATLAB code for FM* [Online]. Available: http://www.circuitsgallery.com/2012/07/matlab-code-for-frequency-modulation-fm.html [Accessed 5 May 2016].
Yates, A. 2008. Elektor FM broadcast super regenerative receiver. Available: http://www.vk2zay.net/article/195.

(Rohde, 2001, Yates, 2008, Fernandez, 2008, Frey, 2013, McFarlane, 1947, McGregor and University of, 2008, Rojas, 1997, Lathi, 1983, Ludwig and Bretchko, 2000, Otung, 2001, King, 1977, Petruzzellis, 2008, Schetgen and American Radio Relay, 1992)

Appendices

Appendix A – Semester 1 Gannt Chart

ID	Task Name	Start	Finish	Duration
1	Receive Brief	12/10/2015	12/10/2015	1d
2	Research SRR	13/10/2015	01/02/2016	80d
3	Simulate RF waves on matlab	13/10/2015	06/11/2015	19d
4	Initial Designs on Multisim	12/10/2015	06/11/2015	20d
5	Assesment 1	29/10/2015	29/10/2015	0d
6	Simulation of self quench on LTSpice	16/11/2015	19/02/2016	70d
7	Research into SRR equations	22/12/2015	04/04/2016	75d
8	Assesment 2	29/01/2016	29/01/2016	0d

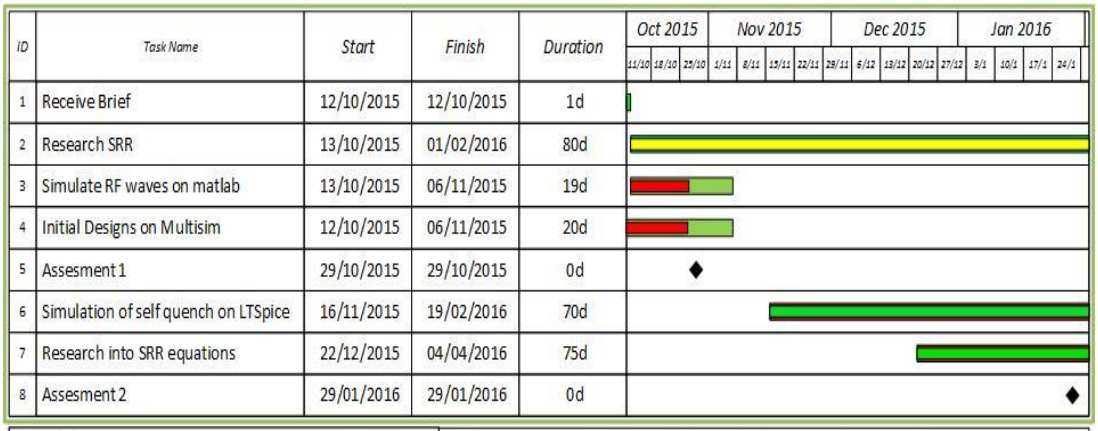

Appendix B – Semester 2 Gannt chart

ID	Task Name	Start	Finish	Duration
1	**Oscillator**	**08/02/2016**	**06/04/2016**	**43d**
2	Simulate oscillator on LTSpice	08/02/2016	17/03/2016	29d
3	Construct oscillator	18/03/2016	25/03/2016	6d
4	Test oscillator	31/03/2016	06/04/2016	5d
5	**Self quenching SRR**	**15/03/2016**	**29/04/2016**	**34d**
6	Simulate Self quenching SRR circuit	15/03/2016	05/04/2016	16d
7	Finalise design for self quenching SRR	06/04/2016	08/04/2016	3d
8	Construct Self quenching circuit	11/04/2016	19/04/2016	7d
9	Test and modify self quenching circuit	21/04/2016	29/04/2016	7d
10	Simulate externally Quenced SRR	01/04/2016	29/04/2016	21d
11	Analyse results of all experimentation	11/04/2016	29/04/2016	15d
12	Produce poster	28/03/2016	20/04/2016	18d
13	Assesment 3: Poster presentation	21/04/2016	21/04/2016	0d
14	**Dissertation**	**08/04/2016**	**06/05/2016**	**20d**
15	Produce rough draft for dissertation	08/04/2016	02/05/2016	17d
16	Produce final draft of dissertation	03/05/2016	05/05/2016	3d
17	Dissertation submission	06/05/2016	06/05/2016	0d
18	Estimated time frame for Viva voce	16/05/2016	20/05/2016	5d

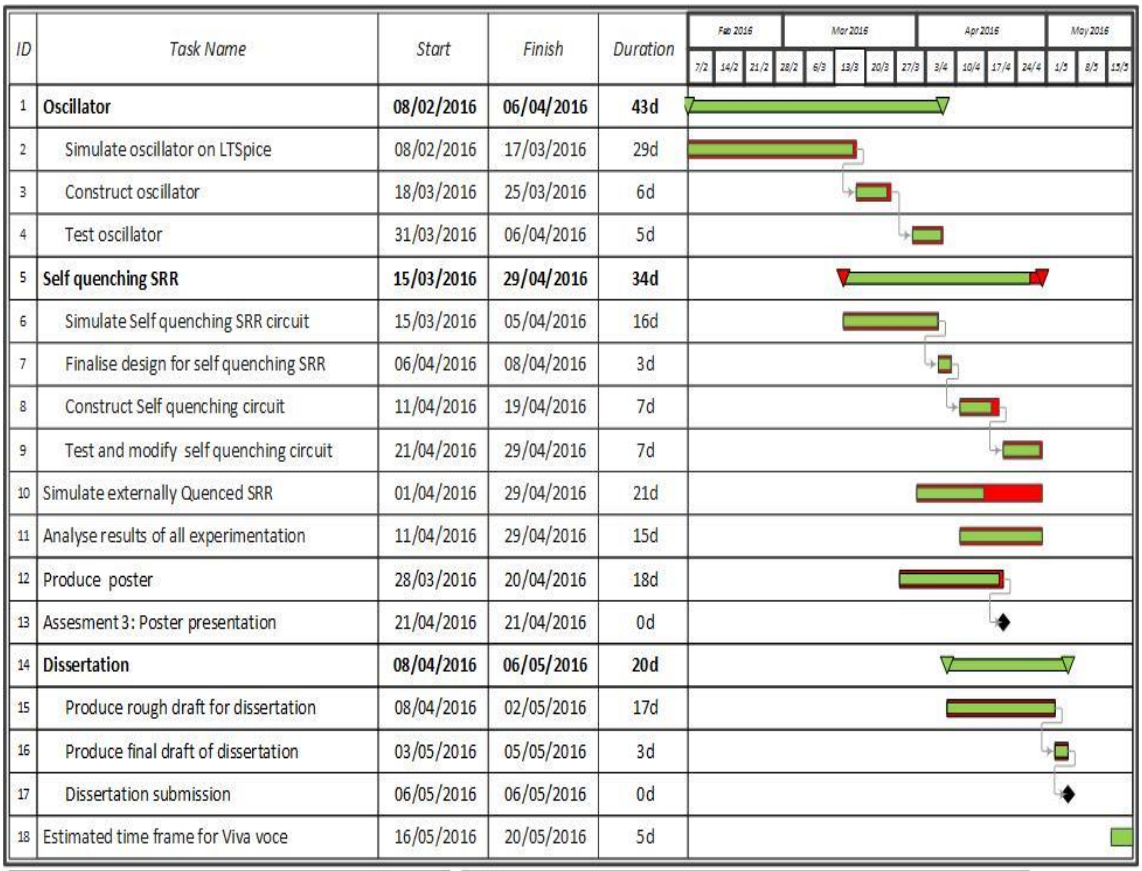

Appendix C- BC 337-25 Transistor parameter curve

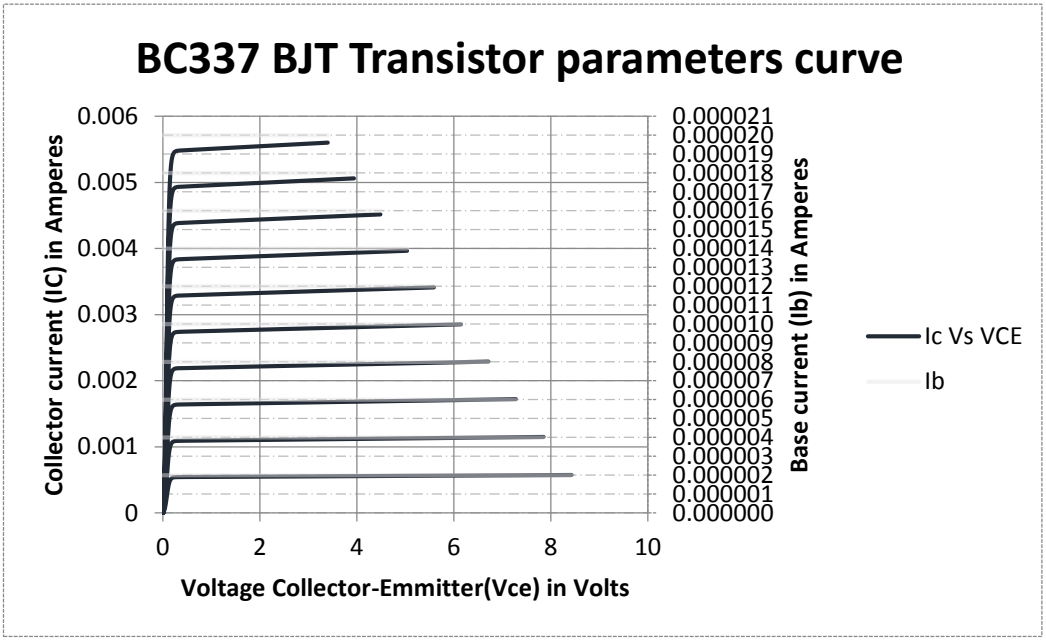

Appendix D-BC547 Transistor parameters curve

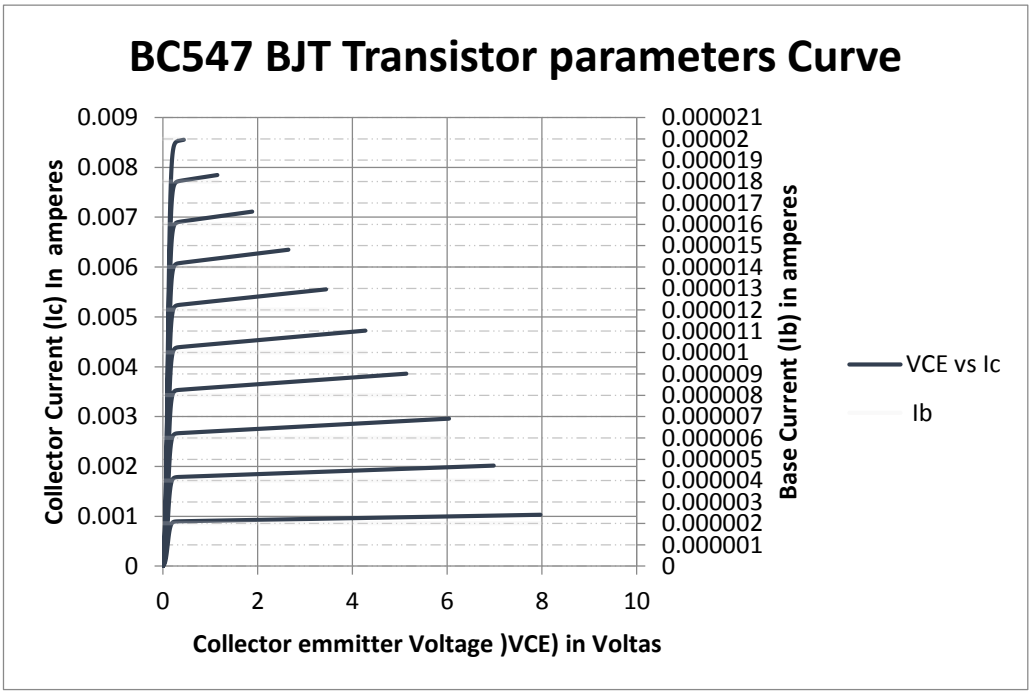

Appendix E- Spice simulation for producing transformer parameters curves

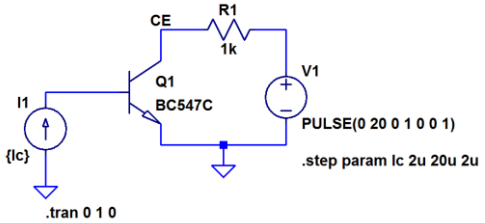

Appendix F-Oscillator DC operating point

---Oscillator DC Operating Point ---		
Parameter	Amplitude	Measurment type
V(vlc1):	9	voltage
V(vb):	4.35855	voltage
V(ve):	3.75666	voltage
V(vc):	8.99825	voltage
Ic(Q1):	0.00079646	device_current
Ib(Q1):	2.83E-06	device_current
Ie(Q1):	-0.0007993	device_current
I(C4):	9.00E-20	device_current
I(C3):	2.46E-22	device_current
I(C2):	1.75E-26	device_current
I(C1):	4.36E-20	device_current
I(L1):	0.00079646	device_current
I(R3):	4.36E-05	device_current
I(R2):	0.00079929	device_current
I(R1):	4.64E-05	device_current
I(V1):	-0.0008429	device_current

Appendix G-SRO DC operating point

Parameter	Amplitude	Measurement type	Parameter	Amplitude	Measurement type
V(vc):	8.99578	voltage	I(C4):	2.96E-25	device_current
V(vb):	4.49661	voltage	I(C3):	3.85E-20	device_current
V(ve):	3.87195	voltage	I(C2):	4.50E-20	device_current
V(vc4):	9	voltage	I(L2):	0.00192634	device_current
V(vout):	3.85269	voltage	I(L1):	-0.0019196	device_current
Ic(Q1):	0.00191956	device_current	I(R3):	0.00449661	device_current
Ib(Q1):	6.78E-06	device_current	I(R2):	0.00192634	device_current
Ie(Q1):	-0.00192634	device_current	I(R1):	0.00450339	device_current
I(C5):	9.00E-20	device_current	I(V1):	-0.006423	device_current
I(C1):	2.41E-22	device_current			

Appendix H-Spice net list for oscillator

```
* G:\Project\SRR_Simulation results\simple_oscillator_06-04-
16.asc
R1 N001 N002 100k
R2 N003 0 4k7
R3 N002 0 100k
```

```
C1 N002 0 10n
C2 N001 Vc 82p
C3 Vc N003 47k
C4 N001 0 10n
Q1 Vc N002 N003 0 BC337-25
L1 N001 Vc 1µ Rser=2.2
V1 N001 0 9
.model NPN NPN
.model PNP PNP
.lib C:\Program Files (x86)\LTC\LTspiceIV\lib\cmp\standard.bjt
.tran 0 0.010 0 0.001
.backanno
.end
```

Appendix I-Spice net list for SRO

```
* G:\Project\Final_Draft_1\Spice schematics\SRR_7-4-
16_self_quench_test.asc
Q1 Vc Vb Ve 0 BC337-25
R1 VC4 Vb 1k
R2 Vout 0 3k
C2 Vb 0 10nF
C3 Vout 0 10nF
L1 Vc VC4 1µ Rser=2.2
C4 VC4 Vc 5p
L2 Ve Vout 33µH Rser=10
V1 VC4 0 9V
R3 Vb 0 1k
C1 Vc Ve 47pF
C5 VC4 0 10n
.model NPN NPN
.model PNP PNP
.lib C:\Program Files (x86)\LTC\LTspiceIV\lib\cmp\standard.bjt
.tran 0 220us 0 10ns
;op
* SRR Super-regenerative Oscillator\nSimulation version
.backanno
.end
```

Appendix J- Spreadsheet for capacitor vs frequency

Capacitance	Multiplier	Pico Farads	Inductance	Multiplier	Micro henries	2pi	sqrt LC	2piSQRT (LC)	f=1/2piSQRTLC
1	1E-12	1E-12	1	0.000001	0.000001	6.283185307	1E-09	6.3E-09	159154943.1
5	1E-12	5E-12	1	0.000001	0.000001	6.283185307	2.24E-09	1.4E-08	71176254.34
10	1E-12	1E-11	1	0.000001	0.000001	6.283185307	3.16E-09	2E-08	50329212.1
15	1E-12	1.5E-11	1	0.000001	0.000001	6.283185307	3.87E-09	2.4E-08	41093629.6
20	1E-12	2E-11	1	0.000001	0.000001	6.283185307	4.47E-09	2.8E-08	35588127.17
25	1E-12	2.5E-11	1	0.000001	0.000001	6.283185307	5E-09	3.1E-08	31830988.62
30	1E-12	3E-11	1	0.000001	0.000001	6.283185307	5.48E-09	3.4E-08	29057584.16
35	1E-12	3.5E-11	1	0.000001	0.000001	6.283185307	5.92E-09	3.7E-08	26902095.46
40	1E-12	4E-11	1	0.000001	0.000001	6.283185307	6.32E-09	4E-08	25164606.05
45	1E-12	4.5E-11	1	0.000001	0.000001	6.283185307	6.71E-09	4.2E-08	23725418.11
50	1E-12	5E-11	1	0.000001	0.000001	6.283185307	7.07E-09	4.4E-08	22507907.9
55	1E-12	5.5E-11	1	0.000001	0.000001	6.283185307	7.42E-09	4.7E-08	21460448.15
60	1E-12	6E-11	1	0.000001	0.000001	6.283185307	7.75E-09	4.9E-08	20546814.8
1	1E-12	1E-12	2	0.000001	0.000002	6.283185307	1.41E-09	8.9E-09	112539539.5
5	1E-12	5E-12	2	0.000001	0.000002	6.283185307	3.16E-09	2E-08	50329212.1
10	1E-12	1E-11	2	0.000001	0.000002	6.283185307	4.47E-09	2.8E-08	35588127.17
15	1E-12	1.5E-11	2	0.000001	0.000002	6.283185307	5.48E-09	3.4E-08	29057584.16
20	1E-12	2E-11	2	0.000001	0.000002	6.283185307	6.32E-09	4E-08	25164606.05
25	1E-12	2.5E-11	2	0.000001	0.000002	6.283185307	7.07E-09	4.4E-08	22507907.9
30	1E-12	3E-11	2	0.000001	0.000002	6.283185307	7.75E-09	4.9E-08	20546814.8
35	1E-12	3.5E-11	2	0.000001	0.000002	6.283185307	8.37E-09	5.3E-08	19022654.13
40	1E-12	4E-11	2	0.000001	0.000002	6.283185307	8.94E-09	5.6E-08	17794063.59
45	1E-12	4.5E-11	2	0.000001	0.000002	6.283185307	9.49E-09	6E-08	16776404.03
50	1E-12	5E-11	2	0.000001	0.000002	6.283185307	1E-08	6.3E-08	15915494.31
55	1E-12	5.5E-11	2	0.000001	0.000002	6.283185307	1.05E-08	6.6E-08	15174828.41
60	1E-12	6E-11	2	0.000001	0.000002	6.283185307	1.1E-08	6.9E-08	14528792.08
1	1E-12	1E-12	3	0.000001	0.000003	6.283185307	1.73E-09	1.1E-08	91888149.24
5	1E-12	5E-12	3	0.000001	0.000003	6.283185307	3.87E-09	2.4E-08	41093629.6
10	1E-12	1E-11	3	0.000001	0.000003	6.283185307	5.48E-09	3.4E-08	29057584.16
15	1E-12	1.5E-11	3	0.000001	0.000003	6.283185307	6.71E-09	4.2E-08	23725418.11
20	1E-12	2E-11	3	0.000001	0.000003	6.283185307	7.75E-09	4.9E-08	20546814.8
25	1E-12	2.5E-11	3	0.000001	0.000003	6.283185307	8.66E-09	5.4E-08	18377629.85
30	1E-12	3E-11	3	0.000001	0.000003	6.283185307	9.49E-09	6E-08	16776404.03
35	1E-12	3.5E-11	3	0.000001	0.000003	6.283185307	1.02E-08	6.4E-08	15531932.06
40	1E-12	4E-11	3	0.000001	0.000003	6.283185307	1.1E-08	6.9E-08	14528792.08
45	1E-12	4.5E-11	3	0.000001	0.000003	6.283185307	1.16E-08	7.3E-08	13697876.53
50	1E-12	5E-11	3	0.000001	0.000003	6.283185307	1.22E-08	7.7E-08	12994946.69
60	1E-12	6E-11	3	0.000001	0.000003	6.283185307	1.34E-08	8.4E-08	11862709.06
1	1E-12	1E-12	4	0.000001	0.000004	6.283185307	2E-09	1.3E-08	79577471.55
5	1E-12	5E-12	4	0.000001	0.000004	6.283185307	4.47E-09	2.8E-08	35588127.17
10	1E-12	1E-11	4	0.000001	0.000004	6.283185307	6.32E-09	4E-08	25164606.05
15	1E-12	1.5E-11	4	0.000001	0.000004	6.283185307	7.75E-09	4.9E-08	20546814.8
20	1E-12	2E-11	4	0.000001	0.000004	6.283185307	8.94E-09	5.6E-08	17794063.59
25	1E-12	2.5E-11	4	0.000001	0.000004	6.283185307	1E-08	6.3E-08	15915494.31
30	1E-12	3E-11	4	0.000001	0.000004	6.283185307	1.1E-08	6.9E-08	14528792.08
35	1E-12	3.5E-11	4	0.000001	0.000004	6.283185307	1.18E-08	7.4E-08	13451047.73
40	1E-12	4E-11	4	0.000001	0.000004	6.283185307	1.26E-08	7.9E-08	12582303.03
45	1E-12	4.5E-11	4	0.000001	0.000004	6.283185307	1.34E-08	8.4E-08	11862709.06
50	1E-12	5E-11	4	0.000001	0.000004	6.283185307	1.41E-08	8.9E-08	11253953.95
60	1E-12	6E-11	4	0.000001	0.000004	6.283185307	1.55E-08	9.7E-08	10273407.4
1	1E-12	1E-12	5	0.000001	0.000005	6.283185307	2.24E-09	1.4E-08	71176254.34
5	1E-12	5E-12	5	0.000001	0.000005	6.283185307	5E-09	3.1E-08	31830988.62
10	1E-12	1E-11	5	0.000001	0.000005	6.283185307	7.07E-09	4.4E-08	22507907.9
15	1E-12	1.5E-11	5	0.000001	0.000005	6.283185307	8.66E-09	5.4E-08	18377629.85
20	1E-12	2E-11	5	0.000001	0.000005	6.283185307	1E-08	6.3E-08	15915494.31
25	1E-12	2.5E-11	5	0.000001	0.000005	6.283185307	1.12E-08	7E-08	14235250.87
30	1E-12	3E-11	5	0.000001	0.000005	6.283185307	1.22E-08	7.7E-08	12994946.69
35	1E-12	3.5E-11	5	0.000001	0.000005	6.283185307	1.32E-08	8.3E-08	12030982.84
40	1E-12	4E-11	5	0.000001	0.000005	6.283185307	1.41E-08	8.9E-08	11253953.95
45	1E-12	4.5E-11	5	0.000001	0.000005	6.283185307	1.5E-08	9.4E-08	10610329.54
50	1E-12	5E-11	5	0.000001	0.000005	6.283185307	1.58E-08	9.9E-08	10065842.42
60	1E-12	6E-11	5	0.000001	0.000005	6.283185307	1.73E-08	1.1E-07	9188814.924